Ecological Engineering 82 (2015) 624–642

Contents lists available at ScienceDirect

Ecological Engineering

journal homepage: www.elsevier.com/locate/ecoleng

A spatially based area–time inundation index model developed to assess habitat opportunity in tidal–fluvial wetlands and restoration sites

André M. Coleman[a,*], Heida L. Diefenderfer[b], Duane L. Ward[a,1], Amy B. Borde[b]

[a] Pacific Northwest National Laboratory, Earth Systems Science Division, Hydrology Technical Group, P.O. Box 999, MSIN K9-33, Richland, WA 99352, USA
[b] Pacific Northwest National Laboratory, Coastal Sciences Division, Marine Sciences Laboratory, 1529 West Sequim Bay Road, Sequim, WA 98382, USA

ARTICLE INFO

Article history:
Received 21 May 2014
Received in revised form 8 April 2015
Accepted 23 May 2015
Available online 17 June 2015

Keywords:
Aquatic terrestrial interface
Connectivity
Environmental flow
Estuary
Hydrological reconnection
Hydropower mitigation
Restoration
Riparian
Salmon
Spatial modeling
Terrain analysis
Tidal hydrology

ABSTRACT

A geographic information system (GIS)-based Area-Time Inundation Index Model (ATIIM) was developed to predict and evaluate availability of hydrologically connected habitats in estuarine and tidal–fluvial regions. The model establishes and describes patterns in the spatial and temporal relationships of the land and water including non-dimensional area–time and volume–time inundation indices. The processing integrates in situ or modeled water-surface elevation (WSE) data with high-resolution elevation data, using established terrain generation and spatial hydrologic analysis methods which are applied in a new geographic domain: the low-relief microtopography characteristic of coastal wetlands. The ATIIM links these data to newly developed, spatially continuous wetted-area algorithms in a GIS module and determines site average bankfull elevation, two- and three-dimensional inundation extent, and other spatial, tabular, and graph-based metrics. It is a cost-effective, rapid assessment tool suitable for the desktop planning environment, and represents an advance over methods that estimate inundation but do not enforce hydrological connectivity. Example model outputs for 11 tidal wetland areas in the lower Columbia River floodplain and estuary illustrate habitat opportunity for threatened and endangered salmon. Outputs for wetland reference sites (tidal marshes and tidal forested wetlands) are compared with river-restoration sites where objectives include increasing salmon access to beneficial habitats by hydrologically reconnecting channels in diked areas of the floodplain. Hydrological process metrics produced by the model, both new and commonly used, support the prioritization of proposed restoration sites, pre-construction planning, and post-construction evaluation. For example, the model can help determine relationships between WSE and habitat opportunity, contrast alternative restoration designs, predict impacts of altered flow regimes, estimate nutrient and biomass fluxes, and provide standardized site comparisons to support effective monitoring of the developmental trajectories of restoration sites.

© 2015 Elsevier B.V. All rights reserved.

1. Introduction

Floodplains represent a biodiverse and dynamic ecotone possessing specific processes attributable to the interface between terrestrial and aquatic ecosystems (Naiman and Décamps, 1997). In river floodplain wetlands, the flow regime is a major determinant of the physical and biological components of the ecosystem (Bunn and Arthington, 2002). In coastal large-river regions, tides induce more complex hydrologic processes (Jay et al., 2015). The flora and fauna are adapted to a complex suite of spatiotemporal interactions between the land and the water (Welcomme, 1979; Junk, 1999), and the re-establishment of a natural hydrological regime is important for ecosystem restoration to succeed (Poff et al., 1997). Spatially explicit modeling of such complex inundation regimes presents a significant interdisciplinary challenge, requiring techniques in geoinformatics and hydrology, and the selection of methods has implications for floodplain ecosystem research and restoration.

The hydrological regime of floodplains has been altered by flow regulation, climate cycles, and channel fragmentation, which have strongly affected many large river systems and fisheries throughout the world (Dynesius and Nilsson, 1994; Mote et al., 2005; Battin et al., 2007). Therefore the strategic reconnection of rivers and floodplains at large scales has been recommended to regain the

* Corresponding author. Tel.: +1 509 372 6077.
E-mail address: Andre.Coleman@pnnl.gov (A.M. Coleman).
[1] Present address: MDU Resources Group, Inc., 8113 W Grandridge Blvd, Kennewick, WA 99336, U.S.A.

http://dx.doi.org/10.1016/j.ecoleng.2015.05.006
0925-8574/© 2015 Elsevier B.V. All rights reserved.

values associated with floodplain ecosystems (Opperman et al., 2009). Hydrological process metrics are important in restoration because fluctuations in water level are controlling factors in the development of ecosystem structure and function. The total area, volume, frequency, duration, and timing of inundation over a wetland restoration site or entire riverscape can provide an index of the floodplain disturbance regime and habitat opportunity, and improve understanding of the rates of ecosystem subsidies such as nutrients, detritus, and biomass, which flux between the floodplain and channel network (White and Pickett, 1985; Toth, 1995; Polis et al., 1997; Welcomme, 2008; Junk, 1999).

The characterization of inundation patterns is particularly challenging in managed tidal river floodplains such as the 234-km lower Columbia River floodplain and estuary (LCRE) on the west coast of North America (Fig. 1). The influence of tides and coastal processes interacts with basin-wide multi-objective hydropower operations, water withdrawals, and the dynamics of seasonal and weather-affected river flows (Jay et al., 2015). In this region, juvenile salmon use shallow estuarine and tidal freshwater habitats to feed and rear (Levings and Bouillon, 1994; Johnson et al., 2015). However, the managed hydrograph and passage barriers (e.g., dikes, culverts, and tide gates) diminish opportunities for fish to enter tidal floodplain wetlands (Bottom et al., 2005). Typical for large rivers globally (Tockner and Stanford, 2002), diking and flow reduction have significantly reduced the shallow-water habitat area available to juvenile salmon (Kukulka and Jay, 2003). Thus, the reconnection of lateral floodplain and estuarine habitat with the main-stem river by breaching dikes and removing or replacing culverts and tide gates is a primary activity of the landscape-scale Columbia Estuary Ecosystem Restoration Program (CEERP) (NMFS, 2008; Diefenderfer et al., 2011).

Several methods to quantify the inundation regime of floodplain wetlands have been reported in the literature. Typical examples include direct measurement of water levels using piezometers for groundwater and pressure gauges for surface water as the basis for stage-discharge curves (e.g., Siebentritt et al., 2004). The hydrological parameters developed from such measurement methods depend on the purpose of the study. For example, patterns of discharge and recharge in groundwater flow have been assessed using piezometers and paired shallow wells to characterize reference wetland hydrological conditions (Ehrenfeld et al., 2003). To predict sediment transport events, Florsheim et al. (2006) calculated flow-duration curves because the process depends on both the magnitude and duration of overbank flooding. Research on salt marshes along the U.S. Gulf of Mexico and the southeastern Atlantic coast produced a flood area index suitable for tidal areas, which factors in duration and extent of flooding from within 10-m of an established marsh edge (Minello et al., 2012). Methods range from the complex and expensive (e.g., hydrodynamic modeling (Silvestri et al., 2004)) to the simple (e.g., the number of months per year in which standing water is observed (Meyer et al., 2008); extracting a single-value inundation surface (NOAA, 2010)). In practice, many coastal restoration planners produce visualizations of inundation by marking up paper maps or using contours from a digital elevation model (DEM) to represent low, average and maximum water levels.

1.1. Rationale for a new model

Existing methods and models provide various levels of complexity for inundation modeling (Bates et al., 2005; Poulter and Halpin, 2008; NOAA, 2010; Savant and McAlpin, 2014). However, none are able to integrate high-resolution spatiotemporal inundation patterns with the types of data and metrics required to assess habitat opportunity on a tidal–fluvial floodplain, enforce hydrologic connectivity, and produce an array of beneficial decision support metrics for stakeholders and restoration practitioners in a practical, cost-effective manner. The Area Time Inundation Index Model (ATIIM) can be characterized as a community-driven model where the features and capabilities developed are a direct result of stakeholder, restoration practitioner, researcher, program manager, etc. communicated needs. For example, restoration program managers need to quantify opportunities for habitat access at existing and proposed wetland restoration sites (Simenstad et al., 2000), assess restoration trajectories (Simenstad and Thom, 1996), quantify the volumetric

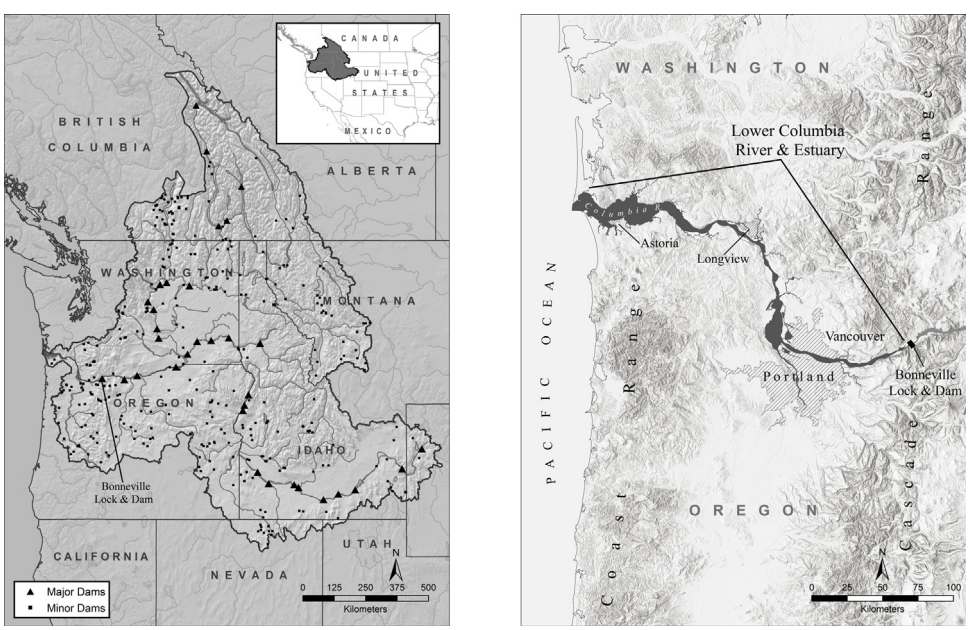

Fig. 1. The Columbia River watershed spans several states within the U.S. and a Canadian province. The hydrologic regime is affected by 32 major dams and approximately 100 minor dams (left). The lower Columbia River and estuary is a 234-km-long tidal–fluvial system and is downriver of all dams (right).

potential for fluxes of allochthonous materials from tidal wetlands to the main-stem river (Polis, 1997), and predict impacts of variable flow regimes (Merritt, 2009), all of which were designed and built into the ATIIM as a result of expressed need. Additionally, numerous potential restoration projects require initial screening and preliminary alternative designs prior to committing significant resources to hydrodynamic modeling, design, and engineering.

In particular, the assessment of habitat opportunity for salmon and other species (Simenstad and Cordell, 2000; Simenstad et al., 2000) is a complex problem in a tidally influenced and hydrologically fragmented riverscape such as the LCRE. The migrations of salmon stocks from throughout the Columbia River basin occur year-round according to diverse life histories and environmental conditions, and all pass through the LCRE prior to entering the ocean (Bottom et al., 2008). The ability of aquatic organisms to access tidal wetland habitats fluctuates dynamically with diel, seasonal and inter-annual differences in the combined tidal and flow regime. The hydrological regime interacts with the channel network morphologies of tidal wetlands on islands and the floodplain; this varies both along the river gradient and laterally from the main-stem river, producing eight hydrologically distinguishable reaches (Jay et al., in revision). These spatially variable and temporally dynamic factors must be assessed together to determine the direct habitat opportunity for salmon stocks and the potential for tidal wetland habitat restoration and resilience; the ATIIM supports this requirement.

1.2. Objectives

The ATIIM is designed for use within estuarine and tidal freshwater environments. It provides spatial and tabular data and metrics describing floodplain terrain and inundation that are not readily available elsewhere while using minimal data inputs and cost-effective methods suitable for rapid-assessment screening. Limited results from earlier versions were presented by Diefenderfer et al. (2008). In its present state, the ATIIM is capable of producing 12 spatial metrics and 30 tabular metrics useful for assessing hydrological and biological conditions and predicting the outcomes of alternative design terrains. Several of these metrics have been found to be particularly useful in restoration planning and evaluation, e.g., hectare-hours of inundation, cumulative frequency of inundation, the area–time inundation index, surface-area to volume ratio, and percent habitat opportunity by elevation and time. At the time of this writing, an additional 20 spatial and tabular metrics are under development and testing to address other properties of the aquatic-terrestrial interface such as vegetation community establishment, shorebird habitat, and impacts from future climates. The model is designed such that functions and metrics can be logically added within the software framework, and efforts are currently underway to make the model publicly available as a geographic information system (GIS) software module.

The key ATIIM design objectives entail (1) rapid assessment of habitat opportunity and capacity for aquatic organisms; (2) capture of microtopography and small channels with dendritic or other patterns in a low-relief riverscape; (3) recognition of hydrological features associated with the contributions of multi-directional flows and the presence of multiple inlet/outlet locations in tidally or fluvially dominated sites; (4) analyses at a resolution suitable for sites 1–500 ha in size; (5) evaluation at varying time scales; (6) comparisons of different sites and the effects of alternative terrain-modification actions; and (7) customization of the model to easily accommodate future metrics.

This paper demonstrates the utility of the new model for rapid assessment and research, and examines its range through applications at 11 sites throughout the LCRE.

2. Methods

In the ATIIM, established terrain-generation and spatial hydrologic-analysis methods are migrated into a low-relief microtopographic domain and integrated with new and existing algorithms to calculate the lateral and vertical propagation of water in tidal-fluvial systems at a high spatiotemporal resolution and produce a suite of spatial, tabular and graph-based metrics (Fig. 2; Table 1).

2.1. Study area

The LCRE is a drowned-river valley characterized by mixed semi-diurnal tides with a 3.6-m or meso-tidal range in the estuary (Sherwood and Creager, 1990). Saltwater intrusion extends to approximately river kilometer (RKM) 20–40, depending on seasonal flows (Jay and Smith, 1990). Though tides affect water levels as far upriver as Bonneville Lock and Dam at RKM 234 (Neal, 1972; Sherwood and Creager, 1990), fluvial influences including hydropower operations dominate the surface water-level regime in the tidal river reaches above RKM 87 (Jay et al., 2015; Jay et al., in revision).

Historically, unregulated Columbia River flows at The Dalles, measured daily since 1878, ranged from a minimum of ~1000 $m^3 s^{-1}$ to a maximum of 35,000 $m^3 s^{-1}$ during spring freshets; the present regulated range is about 2000–16,000 $m^3 s^{-1}$ (Jay et al., 2015). Since the 1930s, the Columbia River's discharge has been increasingly regulated by water withdrawals and the construction and operation of 32 major dams and approximately 100 minor dams in the basin (Fig. 1). In addition to flow regulation, because of an average increase in air temperature of 2.7 °C between 1920 and 2003, as well as a higher density of particulates (e.g., soot, dust) found in the snowpack (Qian et al., 2009; Mantua et al., 2009), the long-term snow water equivalent measured on April 1 has declined from that historically observed in the Pacific Northwest (Mote et al., 2005). Further, the peak spring freshet before 1900 typically occurred in June whereas currently, it occurs in May (Jay et al., 2015). These anthropogenic effects complicate known forcing factors for the downriver hydrograph.

To analyze land-cover changes since 1870, Thomas (1983) used historical data to delineate five habitat types arrayed by elevation in the LCRE: (from highest to lowest) tidal swamp, tidal marsh, shallows and flats, medium-depth water, and deep water. The

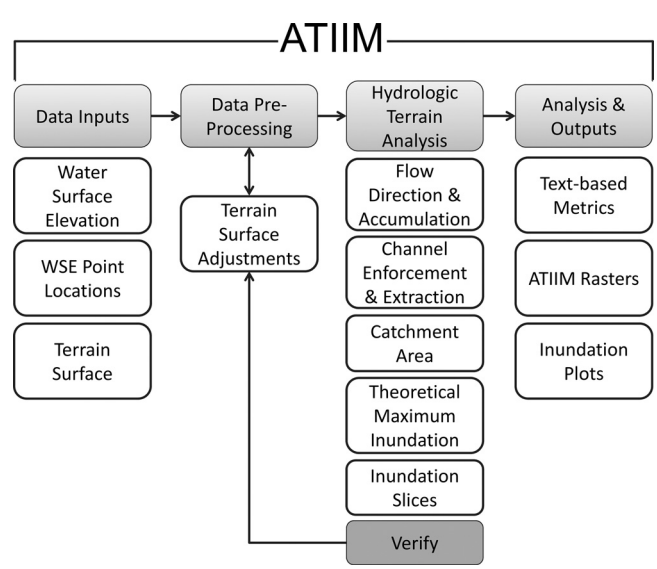

Fig. 2. The workflow sequence in the area–time inundation index model.

Table 1
Standard spatial data products and tabular metrics produced by the ATIIM. Metrics incorporating user-defined elevation intervals were calculated at 0.1-m intervals for this study. The time increment, also user-defined in the ATIIM, was one hour in this study.

Data group	Data	Description
Spatial Data	Surface	Processed and merged LiDAR and bathymetry data with channel enforcement (where LiDAR elevation data are missing due to standing water at the time of data collection)
	Flow accumulation	Raster-based microtopographic flow accumulation for channel routing
	Flow direction	Raster-based microtopographic flow direction for channel routing
	Channels	Microtopographic channel network
	Flow path length	Vector and raster microtopographic channel length
	Channel distance	Raster-based horizontal and vertical distance to defined channels
	Boundaries	Site drainage boundary and micro-basins within the primary site
	Inundation	Data series of two-dimensional wetted area inundation polygons at user-defined elevation increments through the minimum to maximum range of the water-surface elevation record
	Cumulative inundation frequency	Raster-based normalized frequency of inundation
	Volume	Data series of three-dimensional volumetric inundation at user-defined elevation increments through the minimum to maximum range of the water-surface elevation record (provides the basis for calculating nutrient fluxes in the tidal exchange)
	Topographic roughness	Raster-based topographic roughness index (index can be used as a metric for restoration progress and habitat opportunity)
	Topographic wetness index	Raster-based topographic wetness index (index can be used to determine high soil-saturation zones and existing/potential restoration wetlands based on natural topography)
Tabular Metrics	Total time steps	The total number of user-defined time-steps used in the analysis; this value is based on the length of record available from observed water-surface elevations, and in this study, the time-step is hourly
	Days verification	Number of days used in the analysis
	Auto-determined site bankfull elevation (X)	Using an automated graph-based slope-change algorithm, the site average bankfull elevation (X) is determined
	Time steps $<$ inundation elevation of X	The number of time-steps where water remains below the bankfull elevation (X)
	Time steps $\geq$ inundation elevation of X	The number of time-steps where water is present at or above the bankfull elevation (X)
	Percent time $\geq$ bankfull elevation	The percent time (from the total time-series) where water is at or above the bankfull elevation
	Total site area	The total drainage area of the site measured in units of the source data
	Total area-hectares	Total drainage area of the site measured in hectares
	Total hectare-hours	The total number of hectares inundated at each time-step through the study period. Evaluation of inundation occurs at user-defined increments of elevation and time (e.g., hectare-days)"
	Hectare-hours $< X$	The number of hectare-hours below the bankfull elevation (X)
	Percent hectare-hours $< X$	The percent (from the total time-series) of hectare-hours below the bankfull elevation (X)
	Hectare-hours $\geq X$	The number of hectare-hours at or above the bankfull elevation (X)
	Percent hectare-hours $\geq X$	The percent (from the total time-series) of hectare-hours at or above the bankfull elevation (X)
	Theoretical maximum hectare-hour inundation	The theoretical maximum hectare-hour value at the site, assuming the entire site is inundated throughout the entire time-series
	Area-time inundation index	The non-dimensional area-time inundation index is calculated as the number of hectare-hours of inundation, including both in-channel and floodplain area, summed at user-defined increments of elevation, and divided by the theoretical maximum hectare-hours for the site or other user-defined area-time unit
	Volume-time inundation index	The non-dimensional volume-time inundation index is calculated as the volume of water, including both in-channel and floodplain area, summed at user-defined increments of elevation, and divided by the theoretical maximum hectare-meter-hours for the site or other user-defined volume-time unit
	Surface area to volume ratio	Ratio of the planimetric surface area to the three-dimensional volume at each user-defined increment of elevation
	Maximum frequency water-surface elevation (MFWSE)	Most frequently observed water-surface elevation in the period of record
	Habitat opportunity	Data-series of channel edge length habitat availability at user-defined increments of elevation
	Percent habitat opportunity	Data-series of habitat availability at each user-defined increment divided by the total possible habitat availability
	Habitat opportunity at MFWSE	The habitat opportunity percentage at the most frequently observed water-surface elevation in the period of record
	Water-surface elevation percent frequency at bankfull elevation (X)	WSE frequencies greater than or equal to the mean bankfull elevation (can be used as an indicator of the potential frequency with which fish could access emergent marsh habitat)
	Total site channel density	Stream channel length per unit area calculated by dividing the total center-of-channel length at the site by the total site area
	Inundated channel density	Stream channel length per unit area calculated at each user-defined increment of elevation (provides a measure of density in the aquatic/terrestrial interface over varying tidal/flow stages)
	Inundation perimeter	Data series of the total perimeter length of inundated area at each user-defined increment in the WSE data (provides information about aquatic/terrestrial interface characteristics and potential habitat opportunity and flux)
	Inundation perimeter at MFWSE	The inundation perimeter length at the most frequently observed water-surface elevation in the period of record
	Elevation-area relationship (Hypsometric Curve)	Two-dimensional assessment of the landform shape (provides basic metric of opportunity for inundation)
	Site mean topographic roughness index	See description under Spatial Data, above
	Site standard deviation roughness index	See description under Spatial Data, above
	Site mean topographic wetness index	See description under Spatial Data, above
	Site standard deviation wetness index	See description under Spatial Data, above

present study includes models of four Sitka spruce *(Picea sitchensis)* tidal swamps and two tidal marshes, which represent three of the subregions mapped by Thomas (1983): Youngs Bay (RKM 19), Grays River (RKM 34), and Cathlamet Bay (RKM 29) (Fig. 3). These six wetlands are termed reference ecosystems or reference wetlands after SERI (2004), because they are thought to closely represent the ecological conditions intended to result from restoration. Additionally, four restoration sites modelled represent

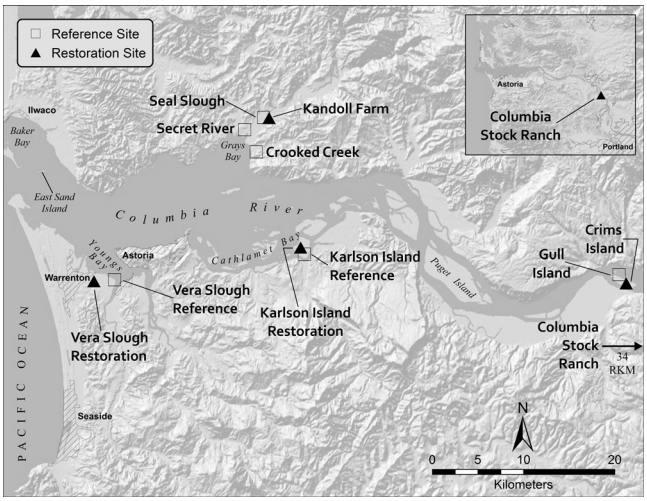

Fig. 3. The 11 study sites in the lower Columbia River and estuary include tidal marsh, forested wetland, and restoration sites.

the range of hydrological reconnection activities occurring in the LCRE; each one is paired with a reference site (Table 2).

The study sites in Youngs Bay include a reference emergent marsh and a wetland that was enhanced by an experimental tide-gate replacement in 2005 (Table 2). The Grays Bay subregion includes three reference tidal forested wetlands and a formerly diked pastureland that underwent dike-breach and culvert-replacement restoration in 2005. The Karlson Island site in Cathlamet Bay has a fourth forested wetland, and an emergent marsh at an unplanned dike-breach restoration dated to sometime between the years 1953 and 1981. Upriver of the Thomas (1983) study area are main-stem island sites including a reference emergent marsh at Gull Island, a wetland restored by channel excavation and scrape-down in 2005 at Crims Island, and a potential restoration site on the south bank, Columbia Stock Ranch, which the authors assessed to demonstrate alternative planning applications of the model.

2.2. Input data

Input data to the ATIIM include the following: (1) a time-series of water surface elevations (WSEs), (2) a high-resolution terrain surface, and (3) the XY coordinate point(s) representing the location of the WSE time-series data (Fig. 2).

2.2.1. Water surface elevation measurements

To document changes in WSEs for reference sites before and after restoration and enhancement actions, absolute pressure sensors were used in reference channels and in channels where culvert installation, tide gate replacement, and dike breaching were to occur (Table 2). The pressure data were recorded hourly and water levels were reported as orthometric heights in the North American Vertical Datum of 1988 (NAVD88) by correcting for atmospheric pressure, incorporating the surveyed top elevation of the instrument casing and static offset distance to the actual sensor. Development of the corrected WSEs allows integration with available high-resolution Light Detection and Ranging (LiDAR) topographic and bathymetric data. Due to environmental circumstances beyond the authors' control and staggered installation of the pressure sensors, all data were not available through the same time periods (Table 2); therefore, to capture similarities and differences between sites, modeling was conducted on a common 150-day time period from February 1 through June 30, 2008 that includes the spring salmon out-migration for the period (Fig. 4). The in situ pressure sensor data used in this study were collected near the outlets of tidal sloughs on the main stem river or on tributaries. Analysis of these data has shown that higher-high water, lower-low water and mean water level at these locations are predictable from main-stem river channel gauge data (Jay et al., in revision) regardless of the microtopography of the wetland. The selection of boundary conditions must fit the study purpose and water-level measurements can and have been used from other sources at various distances from wetland sites of interest, including tide stations, main-stem river 1/2/3D hydrodynamic models, regression-based fluvial tide models (Kukulka and Jay, 2003; Jay et al., in revision), and hypothetical/projected scenarios.

2.2.2. Terrain surface

Using high-resolution ground-surface elevation data (e.g., LiDAR) and specialized terrain processing methods, it is possible to reveal influential microtopographic features, which are particularly important as many estuarine sites exhibit topographic complexity despite minimal landscape relief. This detailed representation of the land surface permits high-resolution horizontal and vertical determination of inundation areas. To gain the highest data value in estuarine systems, traditional topographic LiDAR collections are ideally completed under low-water conditions, thus exposing a greater land surface area. These

Table 2
Study site characterization including dates of collection for WSE data used in modeling.

Site group	Site	Size (km^2)	Characterization	Dates of collection
Youngs Bay	Vera Reference	0.04	Emergent marsh (paired reference)	12/01/2007–06/30/2008
	Vera Slough	1.06	Wetland enhancement w/tide gate replacement (restoration)	04/19/2007–08/20/2009
Grays River	Kandoll Farm	0.66	Formerly diked pastureland (restoration)	07/11/2005–03/10/2008
	Seal Slough	0.08	Sitka spruce swamp (paired reference)	06/10/2005–03/11/2008
	Secret River	0.50	Sitka spruce swamp (reference[a])	07/30/2007–06/29/2008
	Crooked Creek	0.78	Sitka spruce swamp (reference[a])	08/01/2007–07/03/2008
Cathlamet Bay	Karlson Island	3.09	Emergent marsh (unplanned, naturally breached restoration)	8/16/2007–7/20/2008
	Karlson Island	0.15	Sitka spruce swamp (paired reference)	08/16/2007–07/20/2008
Main-stem Columbia River	Crims Island	3.71	Emergent marsh (restoration)	2/13/2008–7/18/2009
	Gull Island	0.10	Emergent marsh (paired reference)	2/13/2008–7/18/2009
	Columbia Stock Ranch[b]	3.90	Wet pasture (restoration is planned)	8/19/2008–8/9/2009

[a] Member of the set of swamp reference sites not paired to a restoration site.
[b] Data used to model the Columbia Stock Ranch were collected at Goat Island.

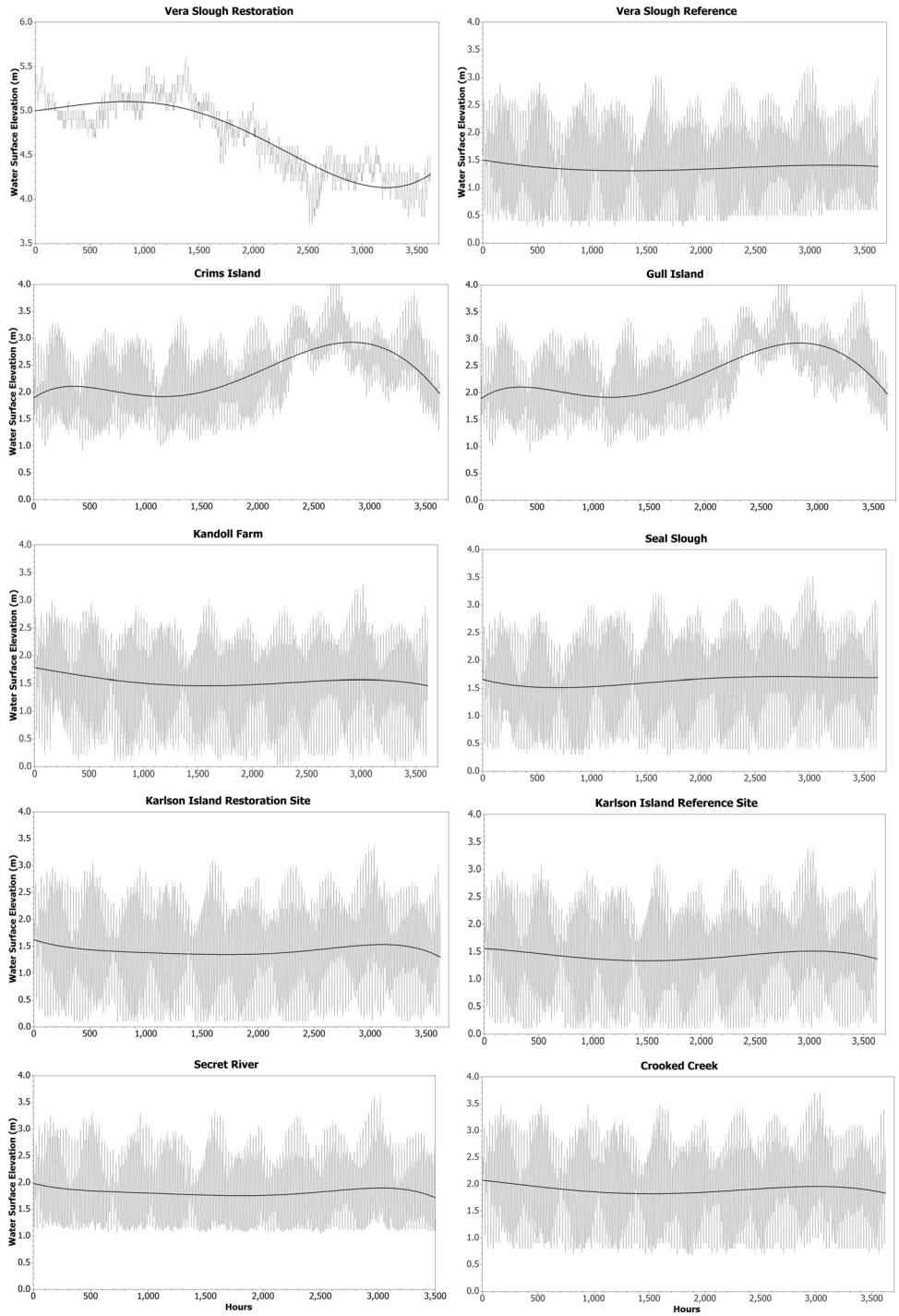

Fig. 4. Hourly flows as recorded and corrected by in situ pressure sensors at 10 study sites for the period from February 1 to June 30, 2008. A fourth-order polynomial fit was applied to each of the data sets to visualize general trends at each site during the primary juvenile salmon out-migration season on the Columbia River.

topographic data can be combined with processed channel cross-section surveys and/or bathymetric surveys to derive a complete terrain surface covering the full inundation flux zone. Alternatively, the use of a green-spectrum laser hydrographic survey LiDAR system (e.g., Compact Hydrographic Airborne Rapid Total Survey system of the U.S. Army Corps of Engineers' Joint Airborne LiDAR Bathymetry Technical Center of Expertise), are capable of simultaneously collecting topographic and bathymetric elevation data (Wozencraft and Millar, 2005; Guenther, 2007).

Elevation data used to create terrain surfaces for all 11 study sites in the LCRE were generated using high-resolution, last-return (i.e., ground-level bare-earth surface) topographic LiDAR data collected in both 2005 and 2009. The data were collected using three different airborne laser terrain-mapping systems: In 2005, the Terrapoint ALTMS 4036 was used, and in 2009, both the Leica ALS50-II and ALS60 were used (PSLC, 2005; USACE, 2013). The LiDAR point-cloud data were collected in a regular grid (2005) and a sinusoidal (2009) scanning pattern with typical ground spacing

between 0.5 and 1.5 m. The LiDAR flight lines included 30–50% sidelap providing data collection at multiple angles, and thus reduced data gaps caused by terrain/object shadowing.

2.3. Data preprocessing: terrain surface adjustments

Preprocessing ground-surface elevation data (merged terrestrial LiDAR and bathymetry) by the ATIIM incorporates a finite difference, locally adaptive terrain algorithm, and terrain surface reconditioning.

2.3.1. Object-relational database

To manage the large LiDAR point cloud data set (~26 billion points) for the terrestrial floodplain areas of the LCRE (Fig. 1), data were imported to a spatially-enabled open-source database (PostGIS/PostGreSQL). Data were retrieved using database queries with user-provided spatial extents. To ensure that drainage areas were captured, the LiDAR data for each site were initially queried and processed for a large extent around the site of interest, aided by the use of high-resolution imagery, high-level hydrologic unit code boundaries (e.g., 10–12 digit codes), and available local- and medium-resolution hydrography data.

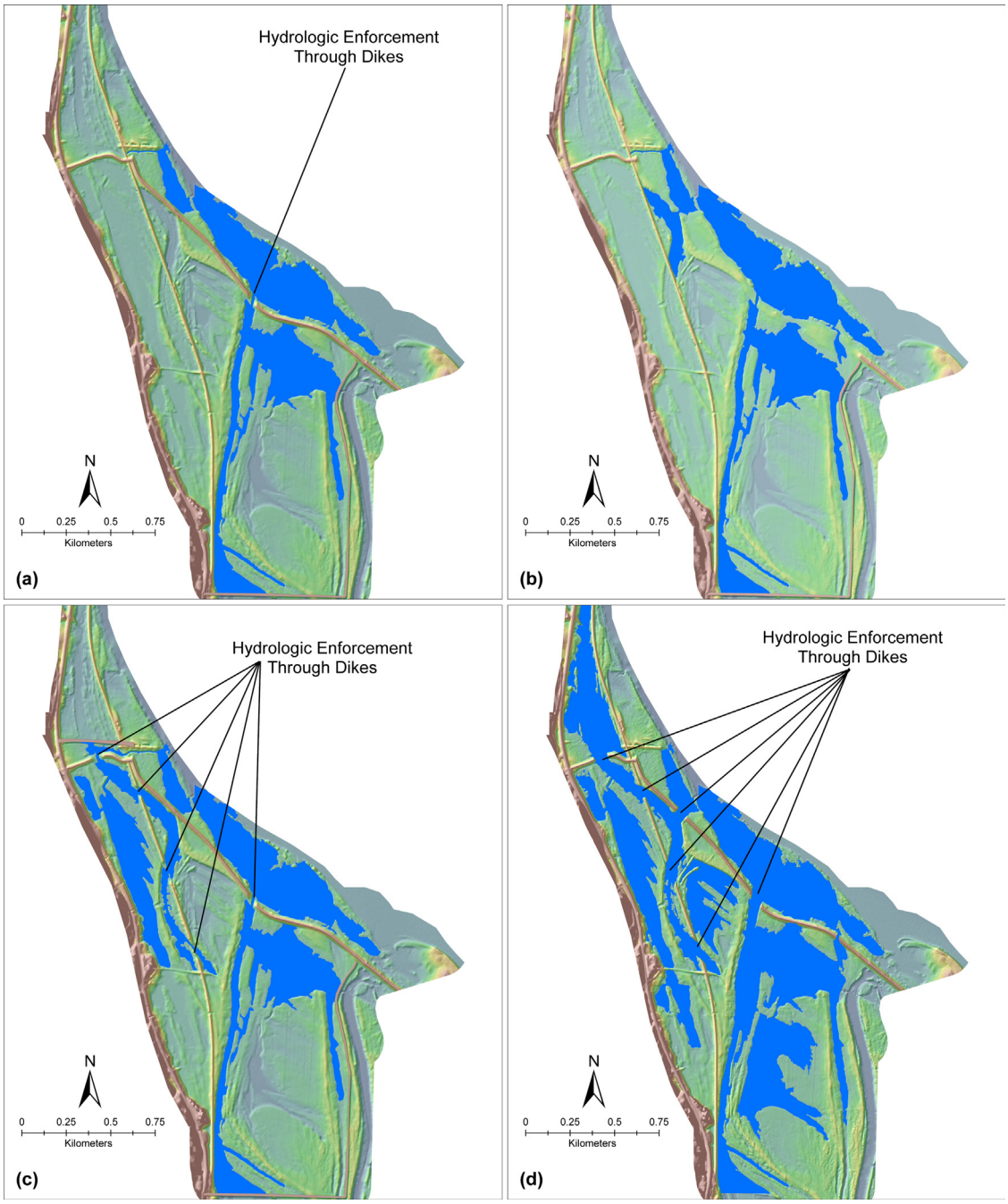

Fig. 5. Four different terrain models for the Columbia Stock Ranch planned restoration site produced after the terrain surface reconditioning algorithm is run on a LiDAR-derived elevation surface. Each terrain represents a different set of identified dike breaches, including a complete dike removal (b). The channel-enforced surface conditioning algorithm effectively dissolves terrain barriers at dike, road, and bridge crossings and is effective for running alternative scenarios for restoration designs. The modeled water surface elevation presented is 4.1 m for all alternatives.

2.3.2. Finite difference, locally adaptive terrain algorithm

The ATIIM incorporates point data from the LiDAR and bathymetric data to produce a continuous high-resolution raster-based terrain surface, using a locally adaptive finite-difference terrain algorithm (Hutchinson, 1989; Hutchinson et al., 2009). The finite-difference algorithm is highly effective for processing multi-scaled complex and low-relief terrain while preserving hydrological integrity by honoring principles of morphometry and hydrological flow. This is accomplished by using terrain roughness penalties and terrain curvature constraints to ensure drainage areas are connected and ridges are preserved. Uncertainty in the source data is factored in to constrain surface modifications of the raw terrain data. Through finite-difference processing of high-resolution terrain data, microtopographic features of the estuarine landscape can be revealed (Moser et al., 2007; Diefenderfer et al., 2008; Courtwright and Findlay, 2011). Other commonly used terrain-generation methods such as nearest-neighbor, kriging, and triangulated irregular networks (TINs) have a tendency to diminish the structure of the microtopography and do not inherently enforce rules of hydrological flow.

In addition to the microtopographic surface providing detail in inundation patterns, it can also reveal many other factors relevant to restoration and research. These include high-resolution and complex channel hydrography to assess habitat availability for quantifying salmon opportunity, terrain roughness (Riley et al., 1999) as a measure of spruce swamp restoration progress (Diefenderfer et al., 2008), valley bottom flatness index for estimating the extent of depositional areas, stream power index to identify erosional areas, and wetness index for understanding patterns of soil moisture and surface water drainage (Boehner et al., 2002; Coleman, 2010).

2.4. Hydrological terrain analysis

Hydrological terrain analysis occurs as an adaptive and iterative loop with the terrain surface adjustments in the ATIIM (Fig. 2).

2.4.1. Channel enforcement

While high-resolution airborne LiDAR data effectively capture tops of dikes, roadways, and bridges, there is no means to represent the open space underneath or through these engineered structures. Therefore, terrain surface reconditioning is used to mathematically warp and trench specific areas through false hydrological barriers represented in the source terrain data. Within the LCRE, these barriers were evidenced by dike breach occurrence after LiDAR collection, tide gates within a diked structure, culverts through built-up roadways, large woody debris in spruce swamp channels (Diefenderfer and Montgomery, 2009), bridge crossings over unimpeded channels, and data anomalies in the source data. Research on digital terrain model channel enforcement has produced many different algorithms over the past two decades (Hutchinson, 1989; Hellweger, 1996; Maidment, 1996; Mizgalewicz and Maidment, 1996; Saunders, 1999; Renssen and Knoop, 2000; Turcotte et al., 2001; Doll and Lehner, 2002; Soille et al., 2003; Hutchinson et al., 2009). The approach taken in this study is distinct in that the drainage-enforced surface reconditioning was only implemented in limited areas where there was a specific need, either because of data representation or restoration planning alternatives involving terrain modification (see Fig. 5).

To resolve false barriers or generate hypothetical removal of barriers, a series of steps is taken and repeated as necessary (Fig. 2). First, using the existing terrain model, data are generated for flow direction, flow accumulation, flow path, and catchment area. Potential barriers are identified using supplemental site imagery, field measurements, and expert knowledge. A manual GIS operation is performed to define polygons around barriers; any elevation data within the polygon are ignored in subsequent terrain processing. Alternatively, individual data points from source elevation data are removed and no longer used in the process. Next, using imagery, flow path data, and flow accumulation data, single or multiple vector lines (distributaries) are generated to delineate the hydrological routes upstream and downstream of barriers. These vectors are used in reprocessing the terrain to enforce hydrological connectivity.

In the case where no bathymetric or channel cross-section data are available, a basic channel geometry is formed in the terrain model using a series of steps (Fig. 6). First, all open-water areas at the time of the LiDAR capture are identified and removed from the source elevation data; for modern LiDAR systems, typically, this information is automatically classified and provided by the data vendor as a separate data file or incorporated into the LASer (LAS) exchange file format. Second, any elevation data from an alternate source is added strictly where open-water data were removed. For

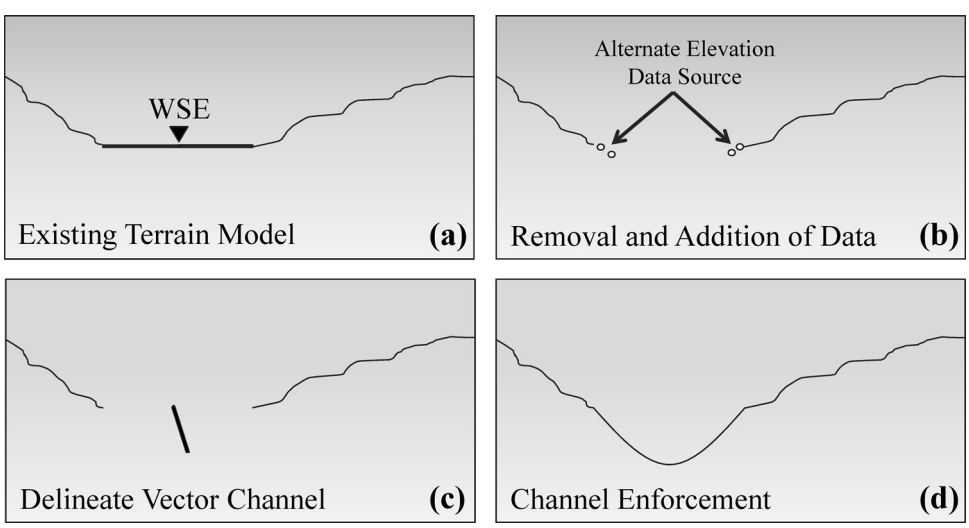

Fig. 6. Terrain model processing involves (a) a high-resolution source digital terrain model with no elevation information beneath the water surface at time of collection; (b) removing elevation data representing the water surface and inserting supplemental data such as channel cross-sections or prior elevation surveys conducted at lower water-surface elevation; (c) delineating the channel center or thalweg (if known) for channel(s) of interest using imagery; and (d) running terrain generation algorithms using updated elevation information and channel vectors to enforce a channel geometry.

example, in the LCRE, a 2005 LiDAR data set flown at a lower tidal-fluvial stage than the 2009 data was used to capture additional near-shore elevation data. Finally, using high-resolution imagery streamline vectors best representing either the channel thalweg or center of channel are manually delineated through the open-water areas. The final channel enforcement is tunable by several parameters, including strength of drainage enforcement, which will impact the channel shape, and relative elevation limits to barriers, which prevent hydrological passage through unrealistically high barriers (Hutchinson, 1989).

2.4.2. Flow direction, accumulation, and path

The deterministic-8 (D8) method (O'Callaghan and Mark, 1984) is commonly used for determining flow direction, flow accumulation, and flow paths. The flow paths travel in one of eight directions separated by 45° angles in the elevation data cell space. While the D8 method is able to achieve good results in areas with well-defined topography and coarser-resolution terrain data, the very subtle topography and abundance of complex micro-channel networks found in estuarine areas, require a more gradient-sensitive approach.

In the ATIIM, raster-based flow accumulation and direction are extracted using the deterministic infinity ($D\infty$) method (Tarboton, 1997) to generate flow direction, flow accumulation, flow paths, and upslope contributing area on the terrain surface. The $D\infty$ method uses a moving 3×3 cell window across the terrain data set. For each data cell, the elevation of the cell center and its eight surrounding neighbors is determined, the individual cells are partitioned into eight planar triangular facets, and each facet is evaluated to determine the slope and direction of steepest descent to identify the next downstream cell, thereby determining overland flow paths through the system (Tesfa et al., 2011). Through this directional process, an accumulation data set is also generated, which maintains a cumulative total of all upstream cells that flow into each cell. The flow accumulation data define points where overland flow converges, leading to the generation of concentrated micro-channel flow paths, eventually scaling to streams and rivers.

The $D\infty$ method avoids and/or minimizes flow dispersion, minimizes grid bias, keeps a high precision of flow direction, and thus develops accurate and representative channel networks (Tarboton, 1997; Tesfa et al., 2011). This method is found to better represent the subtleties of flow direction through low-relief landscapes with complex microtopography. Application of the $D\infty$ method in the tidal wetlands of the LCRE has previously been ground-truthed with good results from Sitka spruce swamps (Diefenderfer et al., 2008).

2.4.3. Catchment area determination: single and multiple drainage outlet points

To determine the drainage outlet point of a site as it connects to the main-stem river, a bay, or a major tributary, a user-defined search radius is provided in the ATIIM to automatically search for the cell with the highest flow accumulation value nearest to the location of the real-world site outlet (the kernel point). This newly defined point location is used to extract the upslope contributing area for the site of interest. Using the flow accumulation matrix, the process steps upstream from the kernel point until flow accumulation is equal to 1 (represents a single cell with no other flow accumulating into it) and continues until all branches have been evaluated. Many estuarine sites differ from traditional watersheds because they can have multiple surface flow inlets and outlets. This can pose a problem for standard hydrological terrain analysis, where surface flow is expected to drain to a single outlet point. For example, at the Vera Slough reference site, a total of 17 separate channels directly enter the adjacent Youngs Bay. The ATIIM accommodates sites with multiple independent channels and corresponding flow entry/exit points. In addition, it makes use of user input, flow direction and flow accumulation data to drive the identification of the outlet points and associated micro-basin boundaries. The resulting drainage boundaries are used to reduce the larger extent terrain data set to only the area that contributes flow to the site—i.e. the hydrological contributing area (Table 1). In addition, the boundaries provide the fundamental computational unit for calculating inundation patterns, after which they are merged to calculate site-wide metrics.

2.4.4. Inundation modeling

The areas of inundation corresponding to WSEs are determined using a GIS-based terrain extraction and channel connectivity algorithm that is based on image segmentation methods developed in remote sensing/image processing (Erikson, 2004; Erikson and Olofsson, 2005). This algorithm uses a kernel point at the basin outlet, extracts the associated WSE and area from the kernel point, then progressively calculates area at user-specified elevation increments through the observed minimum-maximum WSE range. The input elevation range file can easily be modified to evaluate any increment or elevation range relevant to planning or assessment needs. To grow from the kernel while enforcing hydrological connectivity, evaluation of the eight cells adjacent to the center cell takes place repeatedly—cells that meet the criteria are added as the cluster expands through space. The cluster must always move upslope (flow accumulation), cannot proceed past the defined catchment boundary, and must honor matrix Z/elevation values and not exceed the current process-step WSE value.

The resulting spatial analysis calculates the area and volume and provides a lookup table relative to elevation. Frequencies of water-level data for the period of record are generated and related to the user-defined elevation increments. The time-step and elevation increment selected should reflect the data accuracy. All occurrences for each water-level bin are assigned the total inundation area at that level, thereby generating a metric of hectare-hours of inundation, defined by the total area (ha) that is inundated at each time-step and for each WSE increment through the study period (hr). These data provide the basis of most spatial and tabular metrics calculated by the ATIIM model.

2.4.5. Bankfull elevation

Several metrics produced by the ATIIM are influenced by the site average bankfull elevation. Using the graphed inflection point value for the slope of an inundated area or bankfull elevation, the ATIIM segments the hectare-hours of inundation into above and below the bankfull elevation, providing an indication of the site condition. For example, in the absence of engineering controls such as tide gates, some restoration sites in the LCRE are likely to be inundated more frequently than corresponding natural reference sites because of land subsidence behind dikes (Diefenderfer et al., 2008).

To automatically determine the site average bankfull elevation within the model, the methods of Gippell and Stewardson (1998), including maximum curvature and slope, were evaluated; however, for this estuarine system, the values produced were misplaced or required additional data and/or manual interpretation. Therefore, the authors developed a new site average bankfull elevation detection algorithm as part of the ATIIM. The algorithm uses a graph relationship and a hierarchical slope determination between WSE and inundated areas to find the point of inflection, representing the site average bankfull elevation. The bankfull detection algorithm incorporates five primary steps: (1) normalize WSE and inundation area values in a 0–1 range to avoid bias and strengthen maximum slope detection; (2) calculate mean graph

slope within a five-point moving data window; (3) use the mean slope values from each data window to determine the initial greatest change in slope; (4) calculate the slope between each set of two sequential points in the data window with the initial greatest change in slope; and (5) from these, select the point prior to the greatest change in slope as the bankfull elevation and identify the corresponding non-normalized elevation value.

While automated bankfull elevation determination is the objective, the user has the opportunity to review, verify, and change the bankfull elevation value if required. For the 11 sites evaluated, results closely represent what was determined from manual interpretation of the data and observations, with one caveat. We use the term bankfull elevation because it is well-understood, but cross-section surveys and analysis of LiDAR data in Sitka spruce swamps demonstrate that natural levees are formed along the channel banks and natural microtopography is associated with dead wood (Diefenderfer et al., 2008), thus in these ecosystems, the inflection point may not indicate overbank inundation.

2.5. Uncertainty and validation

The modeling of physical processes includes several aspects of uncertainty that need to be considered to establish a level-of-confidence and appropriate uses of the modeled data. For the ATIIM, uncertainty can exist within the WSE inputs, the underlying terrain data, the model formulations and representations, and finally, the model parameters themselves. The WSE data can be sourced from in situ or other modeled data. In the case of in situ WSE data, there is inherent error in the instrument itself, the elevation survey of the instrument, other associated data for processing and correction (i.e., barometric pressure), and the algorithms for processing the raw data to elevations. For modeled WSE data, there are errors in the model and model parameters which vary amongst model types (i.e., hydrodynamic, regression, etc.), the calibration of the model, the boundary conditions used, and errors in the source data inputs. When the ATIIM is used for screening sites where terrain will be modified, in situ data and some modeled data will not reflect the effects of altered micro-topography on water levels and timing so data collected farther from the site may be valuable to provide boundary conditions.

Terrain data can provide a significant source of uncertainty for the ATIIM, though in the case of LiDAR data, this will vary according to topographic complexity, surface roughness, density of vegetation cover, standing water at the time of collection, flight lines, coverage overlap, and the type of LiDAR system used (i.e., terrestrial or hydrographic). For the LCRE, an assessment of the average elevation accuracy for the 2005 LiDAR data is reported at 0.08-m with a root mean square error (RMSE) of 0.11-m based on 10,092 validation points (PSLC, 2005). The elevation accuracy for the 2009 LiDAR data is reported based on a quality control process defined in USACE (2013) where data on open, hard, flat surfaces were assessed for consistency through the full LiDAR collection area. A minimum/maximum absolute elevation accuracy range of 0.01–0.13 m, with an RMSE of 0.046-m was established by evaluating 40,266 ground survey points against the collected LiDAR (USACE, 2013). The accuracy in areas with complex terrain and/or dense or matted vegetation (Hladik and Alber, 2012) will likely be degraded from that reported, however spot checks with in-house surveys indicate final data are within a 0.13-m vertical accuracy and no greater than 0.3-m horizontally.

An assessment of the ATIIM was performed at East Sand Island near the mouth of the Columbia River (RKM 8) at the southern boundary of Baker Bay (Fig. 3). Unfortunately, the field data available for the 11 modeled sites described in this paper focused on other ecological features such as vegetation and fisheries, thus measured water levels were only collected during cross-section surveys at low-tide conditions on infrequent summer site visits and do not reflect broader inundation patterns. At East Sand Island, sub-meter latitude/longitude GPS positions were collected at the water's edge over a two-day period (February 27–28, 2014) representing different locations around the island throughout a 1.2–3.0 m tidal-range. For each GPS position collected, the accompanying LiDAR elevation value was retrieved and compared to the nearest common-time WSE value at the nearest tide station (Hammond, Oregon), approximately 7-km southeast and upstream

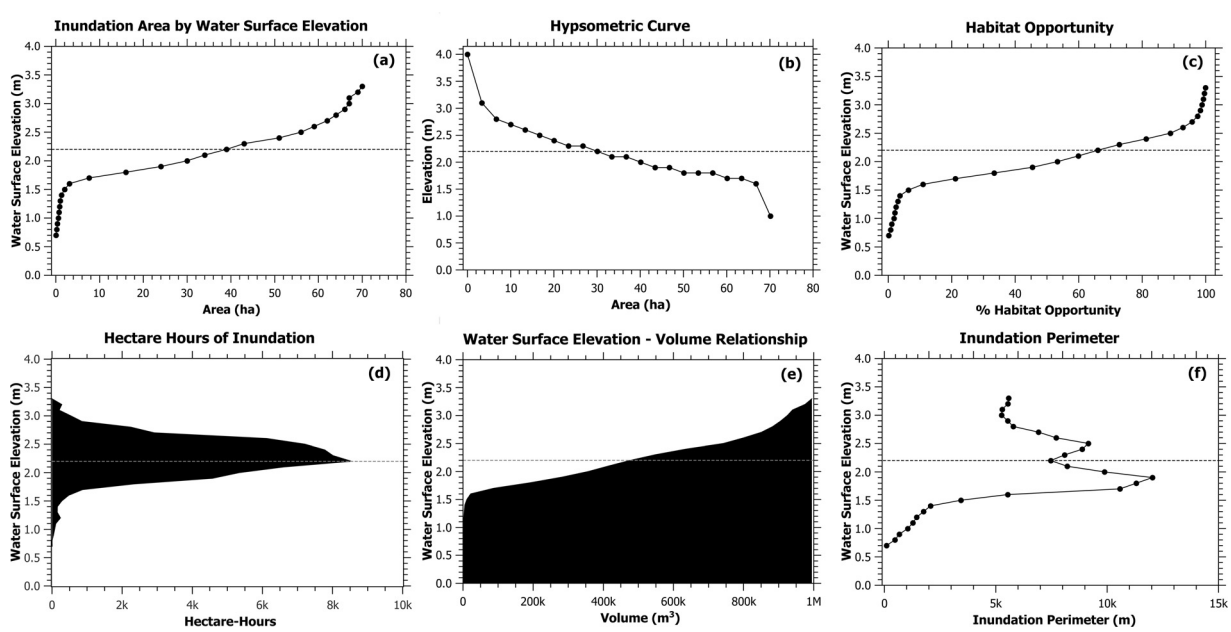

Fig. 7. Example graphical outputs of the ATIIM for the floodplain wetland restoration site, Kandoll Farm, including (a) inundated area by water-surface elevation; (b) hypsometric curve showing the relationship of elevation to total site area; (c) the habitat opportunity by water-surface elevation; (d) total inundation, measured by hectare-hours of the study period for each water-surface elevation; (e) volumetric inundation by water-surface elevation; and (f) the length of channel-edge perimeter by water-surface elevation. The dashed line indicates the most frequently occurring water-surface elevation observed for the time-period.

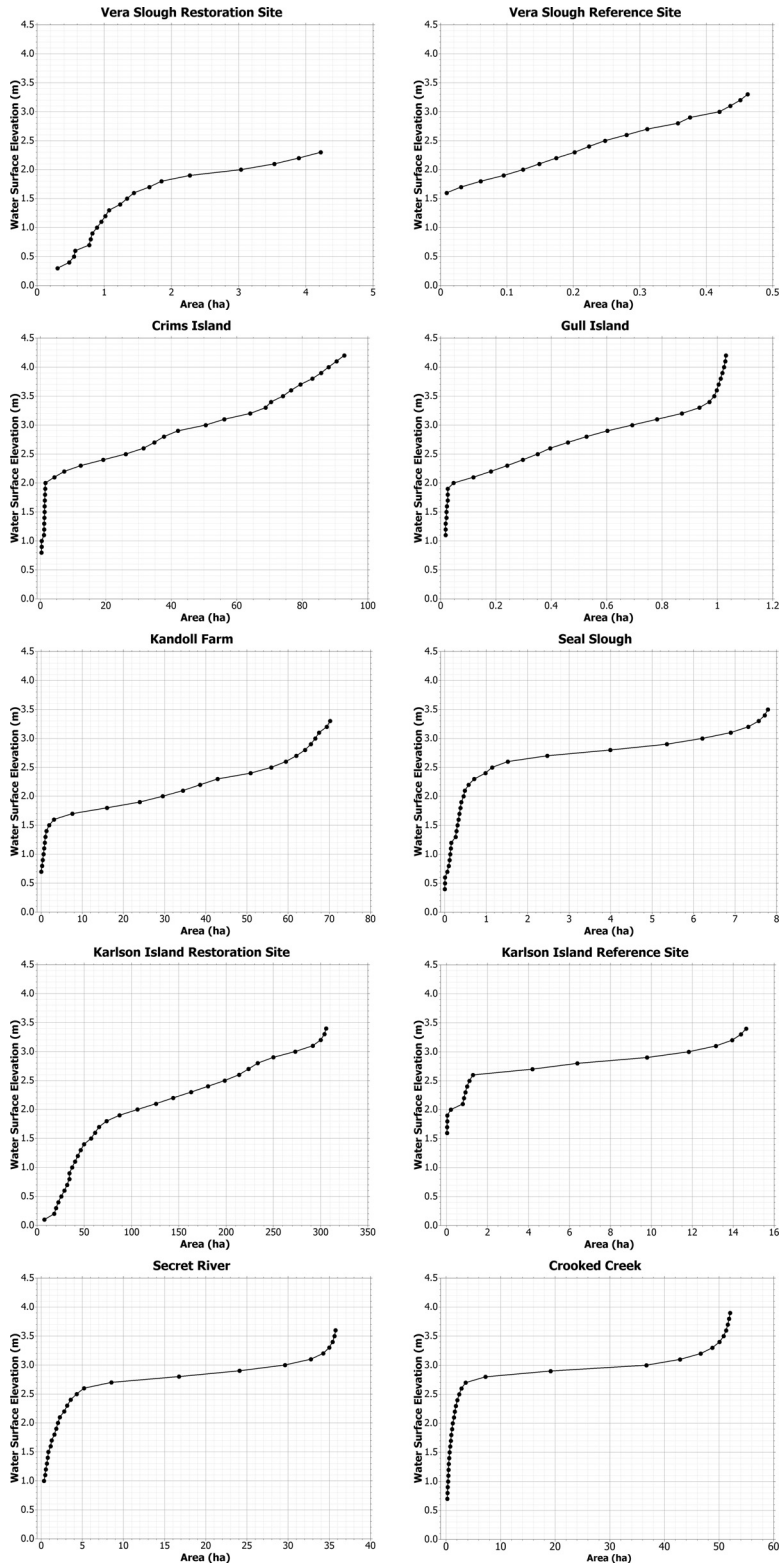

Fig. 8. Water surface elevation-area relationships established for each site by the ATIIM. Note that a clear inflection point is not evident at Vera Slough reference site. Vera Slough restoration site is behind a tide gate and Vera Slough reference site has multiple drainage outlet points.

of East Sand Island. The analysis revealed an average absolute vertical error of 0.15-m with an RMSE of 0.19-m. Using the U.S. National Standard for Spatial Data Accuracy and the National Map Accuracy Standard for vertical accuracy of elevation data, it was determined the 95% confidence interval is 0.38-m, and 0.32-m for the 90% confidence interval (FGDC, 1998). Some of the vertical error can possibly be explained by timing differences of the observed WSE given the 7-km distance of the island relative to the tide station in the lower Columbia River. The average absolute horizontal error between the GPS measured edge-of-water and the ATIIM predicted water's edge is 0.47-m with an RMSE of 0.58-m. The horizontal error is within the margin of error of the GPS measurements and stated LiDAR accuracy. Erosion and depositional changes at East Sand Island could also be reflected in the horizontal error, as the time differential between the LiDAR and GPS validation data is 5-years. Future model validation efforts will incorporate the use of high-accuracy survey methods (e.g., total station, real-time kinematic GPS), on-sight WSE data and/or imaging to further develop model confidence and understand limitations.

A stepping interval analysis was performed to understand the statistical sensitivity, particularly considering vertical uncertainty, of using different elevation increments in the ATIIM. Four representative sites with varying topographic and channel characteristics and total size were selected and tested using four elevation increments between 0.1 and 0.4-m. On average across the sites, statistical results dependent on the automatically-generated bankfull elevation were altered by <4% per 0.1-m increment in elevation; other generated statistics remained unchanged or changed <1%.

2.6. Rapid assessment metrics

The core metric of the ATIIM is the area–time inundation index, calculated as the number of hectare-hours of inundation (A_i), including both in-channel and floodplain area, summed at user-specified increments and divided by the total possible hectare-hours for each site (WSE_{tmax}) Eq. (1).

$$\sum_{i=1}^{n} \frac{A_{i+1}}{WSE_{tmax}} \tag{1}$$

The total possible hectare-hours are determined using (1) the area of the site at two standard deviations above the maximum WSE for the period-of-record and constrained to the site/micro-basin boundary; and (2) the total number of hours in the period-of-record. This provides a theoretical maximum inundation upon which to base the area–time inundation index and importantly, provides a non-dimensional metric that can be used to compare the potential opportunity between individual sites.

Three classes of data output are produced by the ATIIM: (1) spatial data including raster and vector representations of the site under different flow states and restoration designs (Table 1); (2) tabular data providing site characteristics and metrics (Table 1); and (3) graph data derived from the analysis and post-processing of the spatial data (Fig. 7).

2.6.1. Habitat opportunity

While physical inundation patterns provide an important set of metrics for site evaluation, an additional set of decision support metrics are provided that use the physical process representation to quantify potential habitat opportunity for salmon or other species of interest. These site-scale metrics include total channel edge length, percent of accessible channel edge, and channel density at the time-space varying inundation extents to determine the frequency and amount of marsh edge that is accessible to fish for feeding. Habitat opportunity is established with the basic premise that the hydrologic structure on the site will drive opportunity and the underlying basis of the hydrologic structure is the site topography. As a site increases in its WSE as a result of a flow tide, inundation patterns take form, initially following well-established channels then migrating to smaller, less-developed channels, including more subtle inundations through the micro-topography at the upper end of the site or in the floodplain. The calculation of channel edge at the maximum frequency WSE for a given site provides a means of standardizing the amount of available habitat for the size of the site on a unit-area basis.

The extent of habitat at a site can also be evaluated by measuring the total inundation perimeter. This captures islands created by inundation, as well as the complexities in the inundation boundary as a site is responding to ebb and flow tides. Perimeter length at various WSEs can and likely will exceed the total site perimeter because of the representation of inundation complexity at the lower to mid-range WSE. In general, it is expected that the inundation perimeter will recede after a mid-range WSE peak threshold due to a large number of isolated topographic features being inundated and giving way to a single inundation boundary resembling the site boundary. This measure of the aquatic-terrestrial interface provides information about site characteristics and the potential for habitat opportunity and nutrient/biomass flux.

2.6.2. Volumetric calculations

The hydrological regime and geomorphology of a site affect the ability of a reconnected wetland ecosystem to subsidize the food

Table 3
Example calculations performed as a part of the ATIIM are presented for 10 reference and restoration sites. Bankfull elevation is defined by an inundation inflection point as discussed in the text.

	CC	KI	SS	SR	VS	GI	VS[R]	KF[R]	KI[R]	CI[R]
Time-steps (hr)	3625	3624	3625	3593	3623	3624	3623	3612	3624	3624
Total area (ha)	77.6	15.0	7.9	50.0	4.6	1.0	106.0	65.6	308.9	371.4
Bankfull elevation (m, NAVD88)	2.7	2.6	2.5	2.5	1.9	1.9	1.6	1.6	1.8	2.2
Percent time ≥ bankfull elevation	18.7	6.8	14.8	17.4	28.7	74.6	36.1	52.1	37.2	59.4
Total hectare hours	9629	913	1230	7269	1075	574	2659	32668	142170	2617
Hectare hours ≥ bankfull	8064 (83.8%)	607 (66.5%)	745 (60.5%)	5345 (73.5%)	965 (89.7%)	563 (98.2%)	1712 (64.4%)	32149 (98.4%)	98556 (69.3%)	2543 (97.2%)
Hectare hours < bankfull	1565 (16.3%)	306 (33.5%)	486 (39.5%)	1924 (26.5%)	110 (10.3%)	10 (1.8%)	947 (35.6%)	519 (1.6%)	43613 (30.7%)	74 (2.8%)
Max. possible hectare-hour inundation	140680	27232	14219	89247	8384	1869	192132	118473	559734	672922
Area-time inundation index	5.7	2.2	5.2	5.9	11.5	30.1	0.9	27.1	17.6	0.4

Site codes used in the table are as follows: CC: Crooked Creek reference site; KI: Karlson Island reference site; SS: Seal Slough reference site; SR: Secret River reference site; VS: Vera Slough reference site; GI: Gull Island reference site; VS[R]: Vera Slough restoration site; KF[R]: Kandoll Farm restoration site; KI[R]: Karlson Island naturally breached restoration site; CI[R]: Crims Island restoration site.

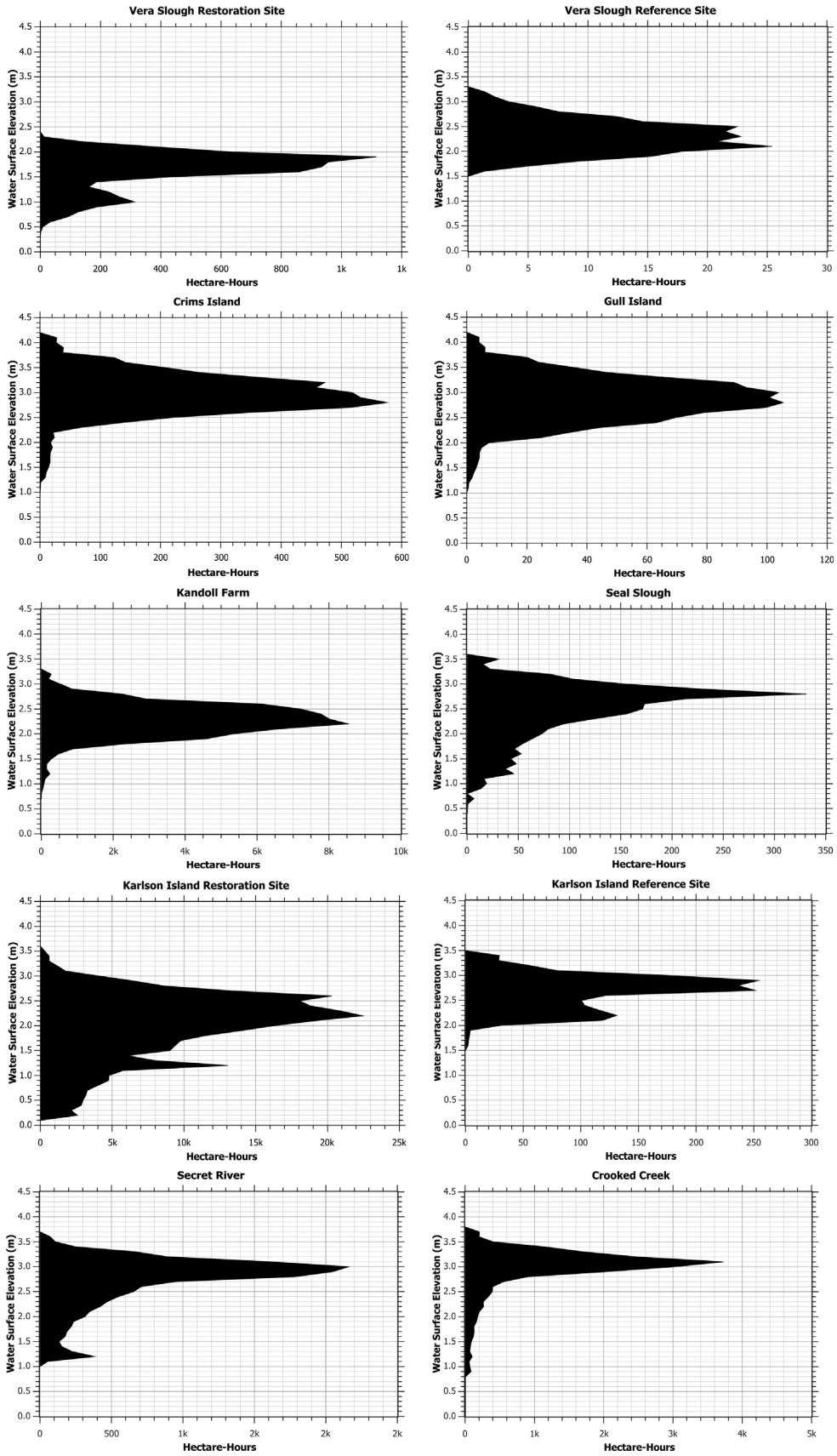

Fig. 9. Total hectare-hours of inundation by water-surface elevation for each of the 10 sites. Note that the area-time inundation index can be influenced by either area or time. The current analysis does not specify the primary driver.

web (Polis et al., 1997), which is an important decision factor in Columbia River salmon recovery (Naiman et al., 2012). Thus, to support researchers in determining the flux of organic matter, nutrients, and detritus-associated invertebrates through ebb and flow cycles at each site, the authors developed the functionality of the ATIIM to calculate a volume time inundation index. The index is calculated as the actual volume of surface water, including both in-channel and floodplain area, summed at user-defined increments of elevation, and divided by the theoretical maximum hectare-meter-hours for the site (Fig. 7e). An associated metric produced by the model is a surface-area-to-volume ratio, defined as the ratio of the planimetric surface area to the 3D volume at each user-specified increment of elevation also helping to provide a predictive measure of flux materials.

The authors also applied these two indices to support fisheries researchers in calculating the volume and surface-area-to-volume ratio of beach seines cast on a tidally influenced island, where the volume of water in a 50-m diameter seine cast from the same point changes continuously and species density metrics are desired. For this application, each seined area is assessed similarly to a site or micro-basin boundary in the model.

3. Results and discussion

The ATIIM analysis results for 11 sites are presented and discussed in several types of research and planning applications to illustrate the utility and range of interpretations that are supported by the model, including comparing restoration and reference sites, evaluating alternative restoration designs, and planning and monitoring restoration actions. Other research applications discussed in Section 2.6 include estimated habitat opportunity and fluxes of nutrients and biomass.

3.1. Comparing restoration and reference sites

This study incorporated two typical reference-site applications used by the programmatic restoration assessment approach for the LCRE (Diefenderfer et al., 2011) where (1) each restoration site was paired with a single reference site to assess restoration targets and monitor change: Vera Slough and Vera Slough reference site, Kandoll Farm and Seal Slough reference site, Crims Island and Gull Island reference site, and the historically breached marsh and reference swamp on Karlson Island; and (2) to broaden understanding of acceptable restoration targets, a group of reference sites was used to evaluate the range of natural conditions in a plant community, in this case Sitka spruce swamps: Seal Slough, Karlson Island, Crooked Creek, and Secret River. Differences among the swamps become evident in the fundamental relationship between WSE and inundated area (Fig. 8). When comparing their topographic settings, it is notable that Secret River and Crooked Creek, located at Grays Bay are perennial streams associated with small upland contributing watersheds. The steeper upland topography of these watersheds does not receive tidal inundation under any conditions observed in this study. Due to the formation of natural channel levees, the inundation inflection point termed bankfull elevation in this study (Fig. 8) occurs below the top-of-bank elevation in Sitka spruce swamps, increasing the modeled values of inundation. Thus interpretations of metrics that

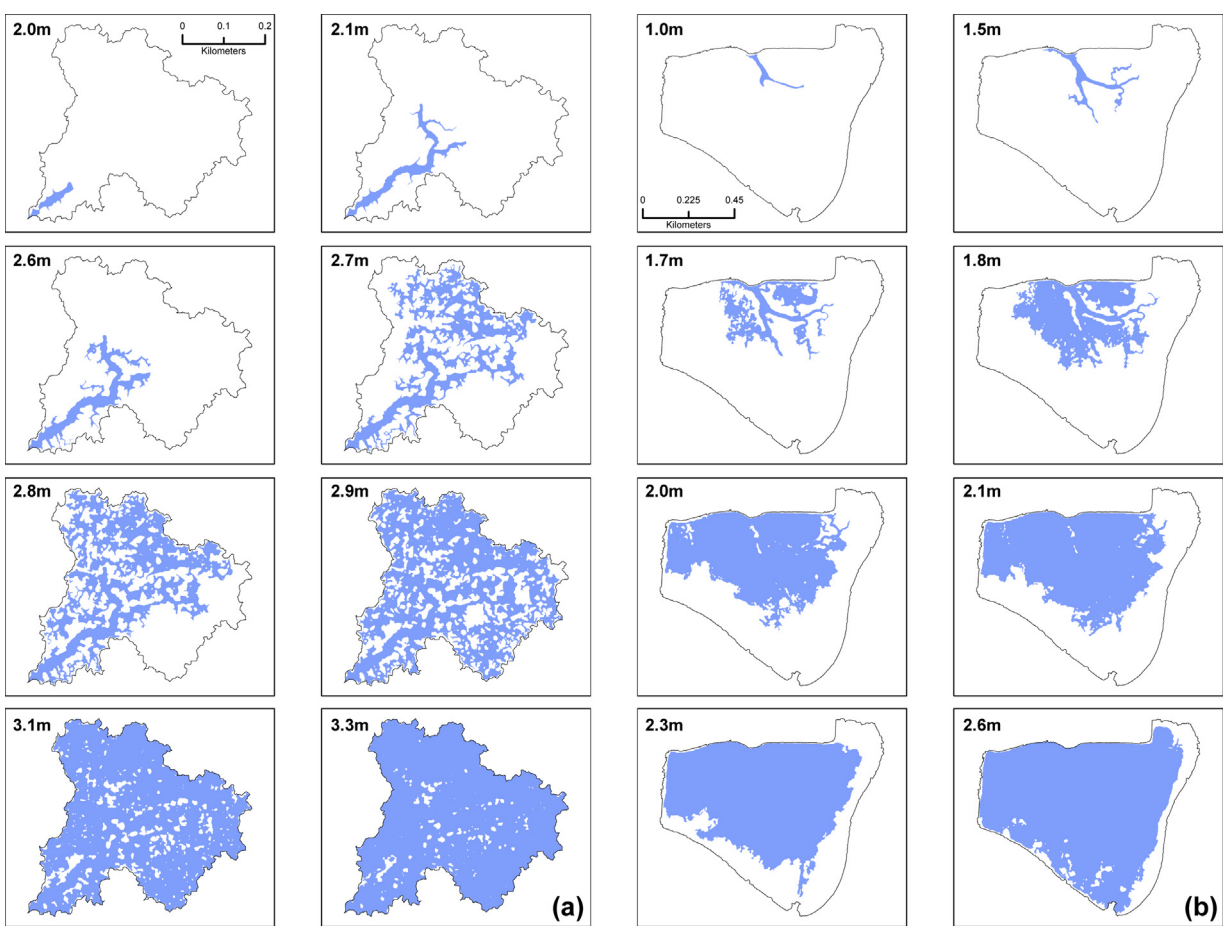

Fig. 10. The inundated areas modeled at multiple water-surface elevations for (a) Karlson Island reference and (b) Kandoll Farm restoration.

incorporate bankfull elevation and particularly any comparisons between swamps and marshes, must consider differences in channel networks and inundation patterns.

Substantial differences between restoration and paired reference sites are seen in the area-time inundation index, frequency of inundation, and other metrics describing the hydrological patterns of each of the 10 restoration and reference sites (Table 3). Visualizing the model outputs and comparing sites includes examining, for each WSE, the total number of hectare-hours of inundation (Fig. 9). Plots of inundated area at multiple WSEs provide a spatial perspective (Fig. 10) showing a 1-m difference in the water elevation required to initiate inundation of two sites. They demonstrate the contrast between the distributed pattern of water propagation throughout the channel network of the Karlson Island reference (Fig. 10a) and the more consolidated expansion front at the marsh restoration site (Fig. 10b). The cumulative frequency of inundation over time highlights the different channel network structures at Vera Slough (single outlet) and its reference site (multiple outlets) (Fig. 11a and b). Likewise, the cumulative frequency of inundation clearly indicates less inundation of the reference site than Kandoll Farm because of diked land subsidence (Diefenderfer et al., 2008) (Fig. 11e and f).

To some extent, variability may be accounted for by the legacies of agricultural land uses at the restoration sites and the

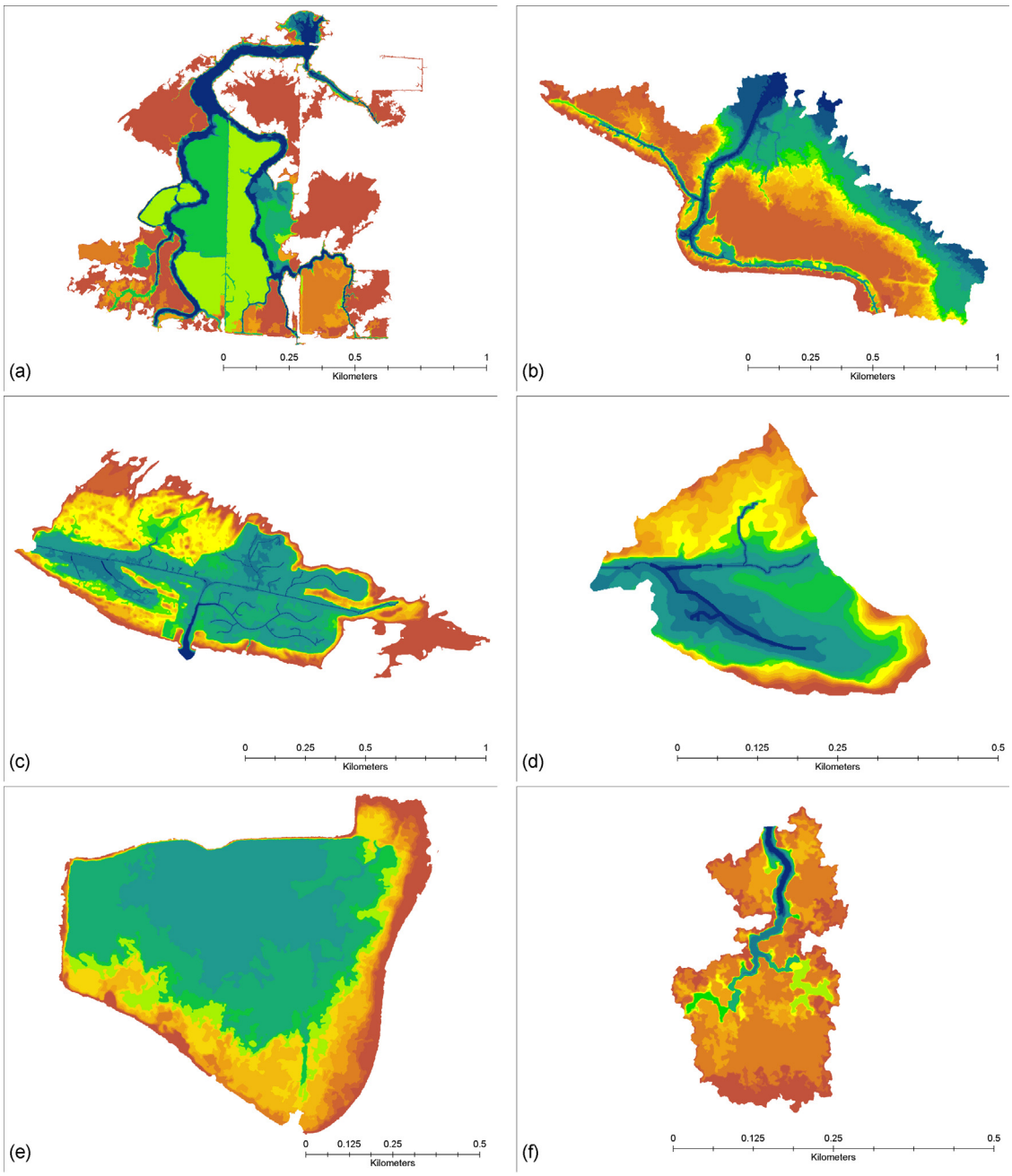

Fig. 11. Cumulative inundation frequency plots for the period of February 1 to June 30, 2008, at 10 study sites: (a) Vera Slough restoration site, (b) Vera Slough reference site, (c) Crims Island restoration site, (d) Gull Island reference site, (e) Kandoll Farm restoration site, (f) Seal Slough reference site, (g) Karlson Island naturally breached restoration site, (h) Karlson Island reference site, (i) Secret River reference site, and (j) Crooked Creek reference site.

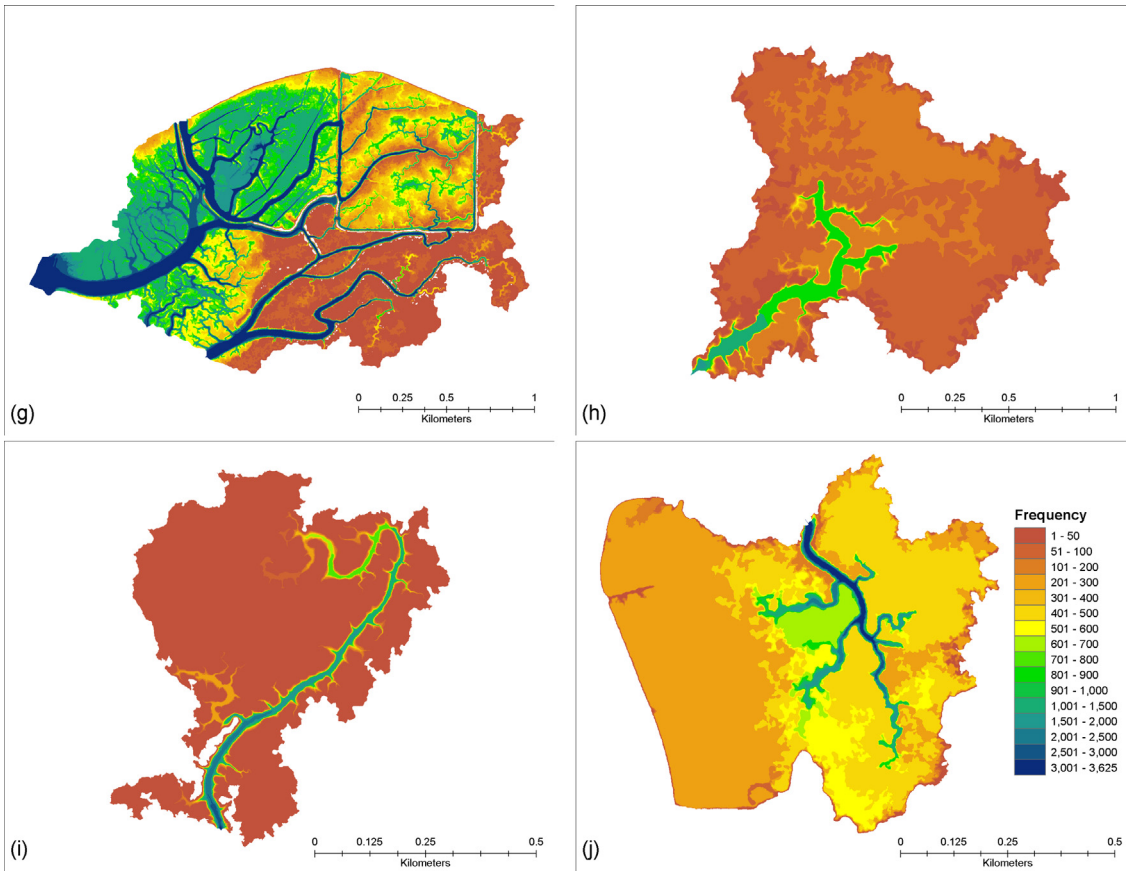

Fig. 11. (Continued)

morphological diversity of tidal channel networks (Rinaldo et al., 2004), especially differences between floodplain microtopography of swamps and marshes. These factors illustrate the challenge of finding hydrologically similar undisturbed reference sites (SERI, 2004). Nevertheless, inter-site comparisons are useful for understanding aquatic and terrestrial habitat structure and the interfaces between them. The cumulative frequency of inundation over time can also help predict plant community development based on the tolerance ranges of individual plant species (Borde et al., 2012) (Fig. 11). The lower inundation frequencies associated with Sitka spruce swamps compared with marshes and restoration sites is clear (Fig. 11f,h,i,j). Following hydrological reconnection to the river, the process of sediment accretion at restoration sites is expected to change the potential plant community from marsh to shrub and finally forest over time.

3.2. Prioritizing restoration sites and alternative actions

Many quantitative approaches have been produced in response to the need to prioritize investments in ecological restoration. Relevant approaches have been variously tailored to focal species (Thompson et al., 2006), ecosystems (e.g., riparian zones (Russell et al., 1997; Timm et al., 2004)), wetlands (Kunert, 2005; Lin et al., 2006), and coastal shorelines (Diefenderfer et al., 2009). Using the methods described herein, functional wetted areas can be modeled prior to consideration for restoration as a screening tool to help understand the potential outcomes of a suite of possible projects and alternative designs, without the significant time-investment involved in the setup, calibration, and running of site-scale 1/2/3D hydrodynamic models. The hydrological regime and topography/bathymetry of a site govern the accessibility of habitat in a reconnected wetland ecosystem to fish (Simenstad et al., 2000). Thus, the authors created multiple terrain surfaces to represent different dike breaching scenarios at a newly acquired restoration site, referred to as the Columbia Stock Ranch (Fig. 5).

The ATIIM was used to examine potential habitat available to stocks of juvenile salmon with different migration timing throughout the year, thus capturing the seasonal changes of river flow and tidal effects under each alternative dike breach or removal scenario (Fig. 5). Over a 178-day period of time, Alternatives A, B, and C provide relatively small differences in the total inundated hectare-hours, ranging from 23,281–26,285 ha-hr and an area-time inundation index ranging from 0.93–1.12, with each alternative successively increasing the amount of inundated area. The design of Alternative D more than triples the amount of inundation, with 90,132 ha-hr over the 178-day time period and roughly doubles the area-time inundation index to 2.20. The index does not necessarily scale similarly as the hectare-hours value given the combination of inundation frequency patterns, area of those inundations and its relation to the theoretical maximum inundation of the site. In all cases, the specific WSE receiving the maximum hectare-hours of inundation is 3.8-m, with Alternatives A, B, and C providing 6323–7,305 ha-hr and Alternative D 17,086 ha-hr, approximately 2.4 times higher than Alternatives A–C. The full dike removal represented in Alternative B is the most costly option and theoretically would enable geomorphological evolution of the floodplain; however, it is minimally effective in terms of the magnitude and duration of inundation.

Table 4
The attributes and limitations of the ATIIM.

ATIIM model attributes	ATIIM model limitations
High-level assessment tool calculating water surface elevations across the landscape at a user-selected time-step; enforces hydrologic connectivity between time-steps	Free-surface/open channel hydraulics are not used
Provides advanced terrain processing and analysis at its core	No velocity calculations are performed
Provides continuous site coverage (2- & 3-dimensional)	Surface water slopes are not considered, which could affect inundation lag times in/out of the site
Provides many features/metrics specific to the microtopography of a site	Ponding effects due to channel constrictions are not considered, which could affect inundation extent and lag times in/out of the site
Includes both vector and raster spatiotemporal analyses	Water quality attributes or transport mechanisms (e.g., temperature, sediment)
Provides spatially explicit suite of metrics for site comparison	
Functions on minimal computer hardware, codes are stable and easy-to-use	
No model calibration requirement	

3.3. Planning and monitoring restoration actions

Practitioners of ecological restoration in transitional ecosystems need new low-cost tools to both predict and measure the effects of management actions on diverse existing and potential hydrological regimes. While the ability to quantify hydrological regimes forms a critical basis for wetland restoration beginning with the early planning phases (Thom et al., 2012), the use of functional hydrological metrics remains necessary during effectiveness monitoring, and finally for adaptive management activities to maximize the achievement of restoration objectives at project and program scales. Effective responses to the call for large-scale prioritization of floodplains for hydrological reconnection (Opperman et al., 2009) depend on the capacity to analyze potential site-scale hydrological regimes relative to flow management of main-stem rivers and other flood controls that prevent lateral connectivity. Moreover, though wetland restoration monitoring programs typically recommend sampling biological and physical metrics including hydrology (Callaway et al., 2001), the monitoring and evaluation of these efforts is often negligible (Bernhardt et al., 2007).

3.4. Limitations and assumptions

As with any model development effort, there are limitations and assumptions that need to be understood so that the end use is appropriate (Table 4). The current assumption of the model is that a discrete WSE is generated at each time-step throughout a study site that does not factor in lag times, potential decay, ponding effects, or surface water slope. Hydrodynamic models can meet these requirements if a study site warrants the need; the ATIIM is designed to provide a less complex rapid assessment capability and can be used to evaluate a site prior to investing heavily in specific designs and/or actions. High-resolution terrain/bathymetry data are ideal for use in an application such as this, but coarser terrain data can also be used to help answer broader-scale questions.

A possible limitation of terrain surface reconditioning as applied by the ATIIM is that elevations, slope values, and all other slope-based data derivatives are likely to exhibit some error in the immediate areas where terrain adjustments are made through hydrologic barriers. This is primarily due to a single delineated channel centerline being used to cut through the barrier, potentially creating steep slopes lateral to the centerline within the immediate vicinity of the artificial terrain barrier. Conversely, a smooth gradient transition is made longitudinally upstream and downstream of the barrier. The objective of this study was to consider the larger terrain surface and ensure replication of existing hydrological connectivity; in this case, the stated limitation associated with the potential terrain error in a highly localized space is not a concern.

While the authors have developed and demonstrated this model on a limited set of restoration and reference sites in the lower part of the LCRE, there is a transition from tidally to fluvially dominated fluctuations over the longitudinal gradient of the Columbia River from the mouth to Bonneville Lock and Dam (Jay et al., 2015). The utility of the method remains to be demonstrated on upper LCRE sites where the influence of hydropower operations is more pronounced. The model itself will function similarly for tidally and fluvially dominated sites provided the basic data requirements are met.

3.5. Future applications and developments

ATIIM-produced metrics can be included as part of multi-objective optimization of flows from upriver dams that not only address accessible habitat, but other objective functions such as power generation, flood control, navigation, water temperature, floodplain agriculture, and dissolved oxygen limits (Gasper et al., 2014). The effects of flow patterns on accessible habitat can be evaluated at characteristic sites that extend through the tidal-fluvial and tidally dominated sections of the LCRE (Jay et al., 2015; Jay et al., in revision). Both observed and optimized flow for the same time period can be used to quantify the system-wide effects and connectivity opportunities as a result of flow optimization. From the salmon recovery perspective, there is a need to define representative flows coming from upriver dams and stratify the effects on downriver shallow-water habitats relative to important annual migration periods and the potential effects of an altered climate (Mote et al., 2005; Battin et al., 2007).

After the implementation of restoration or other management actions, the methods also provide the ability to monitor changes in the developmental trajectories of sites over time to help quantify progress of restoration objectives and forecast future progression. The temporal scales of the model presented here are entirely flexible and may be tailored for research questions concerning the development of multiple biotic structures and processes of interest.

Future developments within the ATIIM include a two-dimensional mass and energy-balance hydraulic modeling engine for optional use to provide further detail of inundation by including cell to cell fluxes that better represent non-linear effects such as inundation diffusion and lag while directly considering bed slope and roughness. This capability can provide flow velocities as well as time-varying water temperature estimates. This development, along with additional field validation of the model under varying hydrologic and inundation conditions at additional sites, will further improve model capability and confidence.

4. Conclusions

The methods described herein, and demonstrated for both restoration sites and reference wetlands at various positions in the tidal floodplain landscape, give researchers a means to rapidly develop comparable functional metrics to describe the hydrological regime that may be applied to hypothetical/alternative scenarios or conditions before and/or after restoration. The ATIIM employs established terrain generation and spatial hydrologic analysis methods, both of which are applied in a new geographic domain (i.e., low-relief, microtopography) to capture hydrologic

features in a manner suitable to the coastal wetland landscape. The model calculates hydrologically connected wetted area and volume and produces a growing list of data and metrics that capture site-scale spatial and temporal inundation patterns. Both new and commonly used metrics are produced by the model, including non-dimensional area-time and volume-time inundation indices, with utility for floodplain and wetland planning, restoration design, research, monitoring and evaluation. The computational requirements of the ATIIM are suitable for rapid assessments in standard desktop environments.

Acknowledgements

This research was partially supported by the U.S. Army Corps of Engineers, Columbia River Fish Mitigation Program (study code EST-02-P-04). The authors thank B. Ebberts, C. Studebaker, G. Johnson, C. Roegner, and R. Thom for management and leadership of the study; the Columbia Land Trust and the Port of Astoria for permission to conduct research on their properties; N. Sather and S. McEwen for contributions to the Columbia Stock Ranch case study; and the many others–particularly R. Kaufmann and S. Zimmerman–who assisted with field data collection.

References

Bates, P.D., Dawson, R.J., Hall, J.W., Horritt, M.S., Nicholls, R.J., Wicks, J., Hassan, M.A. A.M., 2005. Simplified two-dimensional numerical modeling of coastal flooding and example applications. Coastal Eng. 52, 793–810.

Battin, J., Wiley, M.W., Ruckelshaus, M.H., Palmer, R.N., Korb, E., Bartz, K.K., Imaki, H., 2007. Projected impacts of climate change on salmon habitat restoration. PNAS 104 (16), 6720–6725.

Bernhardt, E.S., Sudduth, E.B., Palmer, M.A., Allan, J.D., Meyer, J.L., Alexander, G., Follstad-Shah, J., Hasssett, B., Jenkinson, R., Lave, R., Rumps, J., Pagano, L., 2007. Restoring rivers one reach at a time: results from a survey of U.S. river restoration practitioners. Restor. Ecol. 15, 482–493.

Boehner, J., Koethe, R., Conrad, O., Gross, J., Ringeler, A., Selige, T., 2002. Soil regionalisation by means of terrain analysis and process parameterisation. In: Micheli, E., Nachtergaele, F., Montanarella, L. (Eds.), Soil Classification 2001. European Soil Bureau, Luxembourg, pp. 213–222 Research Report No. 7, EUR 20398 EN.

Borde, A.B., Diefenderfer, H.L., Cullinan, V.I., Thom, R.M., Zimmerman, S.A., 2012. Wetland Reference Sites in the Lower Columbia River and Estuary: Data Synthesis and Restoration Planning Actions. U.S. Army Corps of Engineers 2012 Anadromous Fish Evaluation Program review, Portland, Oregon http://www.nwd-wc.usace.army.mil/tmt/documents/AFEP/Presentation/EST-6_Borde_Wetland-Reference-Sites.

Bottom, D.L., Simenstad, C.A., Burke, J., Baptista, A.M., Jay, D.A., Jones, K.K., Casillas, E., Schiewe, M.H., 2005. Salmon at River's End: The Role of the Estuary in the Decline and Recovery of Columbia River Salmon. NOAA Technical Memorandum NMFS-NWFSC-68, U.S. Department of Commerce, National Oceanic and Atmospheric Administration, Northwest Fisheries Science Center, Seattle, Washington.

Bottom, D.L., Anderson, G., Baptista, A., Burke, J., Burla, M., et al., 2008. Salmon Life Histories, Habitat, and Food Webs in the Columbia River Estuary: An Overview of Research Results, 2002–2006. U.S. Army Corps of Engineers, Portland District, Northwest Division, Portland, Oregon; and Bonneville Power Administration, Environment, Fish, and Wildlife Division, Portland, Oregon, by the Northwest Fisheries Science Center, National Marine Fisheries Service, Seattle, Washington.

Bunn, S., Arthington, A., 2002. Basic principles and ecological consequences of altered flow regimes for aquatic biodiversity. Environ. Manage. 30, 492–507.

Callaway, J.C., Sullivan, G., Desmond, J.S., Williams, G.D., Zedler, J.B., 2001. Assessment and monitoring. In: Zedler, J.B. (Ed.), Handbook for Restoring Tidal Wetlands. CRC Press, Boca Raton, Florida.

Coleman, A.M., 2010. Terrain Analysis Methods Supporting Land Cover Classification for Snohomish County Critical Area Monitoring. PNWD-4145. Battelle–Pacific Northwest Division, Richland, Washington.

Courtwright, J., Findlay, S.E.G., 2011. Effects of microtopography on hydrology, physicochemistry, and vegetation in a tidal swamp of the Hudson River. Wetlands 31, 239–249.

Diefenderfer, H.L., Montgomery, D.R., 2009. Pool spacing, channel morphology, and the restoration of tidal forested wetlands of the Columbia River, U. S. A. Restor. Ecol. 17, 158–168.

Diefenderfer, H.L., Coleman, A.M., Borde, A.B., Sinks, I.A., 2008. Hydraulic geometry and microtopography of tidal freshwater forested wetlands and implications for restoration, Columbia River, U. S. A. Ecohydrol. Hydrobiol. 8 (2–4), 339–361. doi: http://dx.doi.org/10.2478/v10104-009-0027-7.

Diefenderfer, H.L., Sobocinski, K.L., Thom, R.M., May, C.W., Borde, A.B., Southard, S.L., Vavrinec, J., Sather, N.K., 2009. Multiscale analysis of restoration priorities for marine shoreline planning. Environ. Manage. 44, 712–731.

Diefenderfer, H.L., Thom, R.M., Johnson, G.E., Skalski, J.R., Vogt, K.A., Ebberts, B.D., Roegner, G.C., Dawley, E.M., 2011. A levels-of-evidence approach for assessing cumulative ecosystem response to estuary and river restoration programs. Ecol. Restor. 29, 111–132.

Doll, P., Lehner, B., 2002. Validation of a new global 30-min drainage direction map. J. Hydrol. 258 (1–4), 214–231.

Dynesius, M., Nilsson, C., 1994. Fragmentation and flow regulation of river systems in the northern third of the world. Science 266 (5186), 753–762.

Ehrenfeld, J.G., Bowman Cutway, H., Hamilton IV, R., Stander, E., 2003. Hydrologic description of forested wetlands in northeastern New Jersey, USA—an urban/suburban region. Wetlands 23, 685–700.

Erikson, M., Olofsson, K., 2005. Comparison of three individual tree crown detection methods. Mach. Vision. Appl. 16 (4), 258–265.

Erikson, M., 2004. Species classification of individual segmented tree crowns in high resolution aerial images using radiometric and morphologic image measures. Remote Sens. Environ. 91 (3–4), 469–477.

Florsheim, J.L., Mount, J.F., Constantine, C.R., 2006. A geomorphic monitoring and adaptive assessment framework to assess the effect of lowland floodplain river restoration on channel-floodplain sediment continuity. River Res. Appl. 22, 353–375.

Federal Geographic Data Committee (FGDC), 1998. Geospatial Positioning Accuracy Standards Part 3: National Standard for Spatial Data Accuracy, FGDC-STD-007.3-1998, 28p.

Gasper J.R., Veselka T.D., Mahalik M.R., Hayse J.W., Saha S., Wigmosta M.S., Voisin N., Rakowski C.L., Coleman A.M., Lowry T.S., 2014. Water Use Optimization Toolset Project: Development and Demonstration Phase Draft Report, Argonne National Laboratory, ANL/EVS-14/5.

Gippell, C.J., Stewardson, M.J., 1998. Use of wetted perimeter in defining minimum environmental flows. Regulated Rivers: Res. Manage. 14, 53–67.

Guenther, G.C., 2007. In: Maune, D. (Ed.), Digital Elevation Model Technologies and Applications: The DEM Users Manual. 2nd Edition American Society for Photogrammetry and Remote Sensing, pp. 253–320 Chapter 8: Airborne lidar bathymetry.

Hellweger, R., 1996. AGREE–DEM Surface Reconditioning System. Center for Research in Water Resources. The University of Texas at Austin, Austin, Texas http://www.ce.utexas.edu/prof/maidment/gishydro/ferdi/research/agree/agree.html.

Hladik, C., Alber, M., 2012. Accuracy assessment and correction of a LiDAR-derived salt marsh digital elevation model. Remote Sens. Environ. 121, 224–235.

Hutchinson, M.F., Stein, J.A., Stein, J.L., Xu, T., 2009. Locally adaptive gridding of noisy high resolution topographic data. Proceedings of the 18th World IMACS/MODSIM Congress. Elsevier, Amsterdam, The Netherlands.

Hutchinson, M.F., 1989. A new method for gridding elevation and streamline data with automatic removal of pits. J. Hydrol. 106, 211–232.

Jay, D.A., Smith, J.D., 1990. Circulation, density distribution and neap-spring transitions in the Columbia River Estuary. Prog. Oceanogr. 25, 81–112.

Jay, D.A., Leffler, K., Diefenderfer, H.L., Borde, A.B., 2015. Tidal-fluvial and estuarine processes in the lower Columbia River: I. Along-channel water level variations, Pacific Ocean to Bonneville Dam. Estuar. Coasts 38, 415–433.

Jay, D.A., Borde, A.B., Diefenderfer, H.L., (In revision). Tidal-fluvial and estuarine processes in the Lower Columbia River: II. Water level models, floodplain wetland inundation, and reach classification. Estuaries and Coasts.

Johnson, G.E., Ploskey, G.R., Sather, N.K., Teel, D.J., 2015. Residence times of juvenile salmon and steelhead in off-channel tidal freshwater habitats, Columbia River, USA. Can. J. Fish. Aquat. Sci. 72 (1–1) .

Junk, W.J., 1999. The flood pulse concept of large rivers: learning from the tropics. Archiv fur Hydrobiologie 115, 261–280.

Kukulka, T., Jay, D.A., 2003. Impacts of Columbia River discharge on salmonid habitat: 2. Changes in shallow-water habitat. J. Geophys. Res. 108 (C9), 3294.

Kunert, K., 2005. A GIS approach to habitat restoration site selection and prioritization in the New York-New Jersey harbor estuary. Master's Thesis. Duke University, Durham, North Carolina.

Levings, C.D., Bouillon, D., 1994. Estuarine and ocean survival of northeastern Pacific salmon. NOAA Technical Memorandum, NOAA-NMFS-NWFSC TM-29. U.S. Department of Commerce, National Oceanic and Atmospheric Administration, Northwest Fisheries Science Center, Seattle, Washington.

Lin, J.P., Bourne S.G., Kleiss B.A., (2006). Creating a wetland restoration decision support system using GIS tools. Report No. ERDC TN-EMRRP-EM-05, U.S. Army Corps of Engineers, Engineer Research and Development Center, Vicksburg, Mississippi.

Maidment, D., 1996. GIS and hydrological modelling: an assessment of progress. Third International Conference on GIS and Environmental Modelling. National Center for Geographic Information and Analysis, University of California, Santa Barbara, California.

Mantua, N., Tohver, I., Hamlet, A., 2009. Impacts of climate change on key aspects of freshwater salmon habitat in Washington State. Chapter 6 in The Washington Climate Change Impacts Assessment: Evaluating Washington's Future in a Changing Climate. Climate Impacts Group, University of Washington, Seattle, Washington.

Meyer, C.K., Whiles, M.R., Baer, S.G., 2008. Plant community recovery following restoration in temporally variable riparian wetlands. Restor. Ecol. 18, 52–64.

Minello, T.J., Rozas, L.P., Baker, R., 2012. Geographic variability in salt marsh flooding: patterns may affect nursery value for fishery species. Estuaries and Coasts 35, 501–514.
Mizgalewicz, P.J., Maidment, D., 1996. Modelling Agrichemical Transport in Midwest Rivers Using Geographic Information Systems. Online Report 96-6. Centre for Research in Water Resources, University of Texas, Austin, Texas.
Moser, K., Ahn, C., Noe, G., 2007. Characterization of microtopography and its influence on vegetation patterns in created wetlands. Wetlands 27, 1081–1097.
Mote, P.W., Hamlet, A.F., Clark, M.P., Lettenmaier, D.P., 2005. Declining mountain snowpack in western North America. Bull. Am. Meteorol. Soc. 86 (1), 39–49.
National Marine Fisheries Service (NMFS), 2008. Biological opinion–consultation on remand for operation of the federal columbia river power system. 11 Bureau of Reclamation Projects in the Columbia Basin and ESA Section 10(a)(1)(A) Permit for Juvenile Fish Transportation Program. National Oceanic and Atmospheric Administration Fisheries-Northwest Region, Seattle, Washington.
Naiman, R.J., Décamps, H., 1997. The ecology of interfaces: riparian zones. Annu. Rev. Ecol. Systematics 28, 621–658.
Naiman, R.J., et al., 2012. Developing a broader scientific foundation for river restoration: Columbia River food webs. PNAS 109 (52), 21201–21207.
National Oceanic and Atmospheric Administration (NOAA), 2010. Technical considerations for use of geospatial data in sea level change mapping and assessment. Silver Spring, Maryland, NOAA National Ocean Service, NOAA Technical Report NOS 2010–01, 130p.
Neal, V.T., 1972. Physical aspects of the Columbia River and its estuary. In: Pruter, A. T., Alverson, D.L. (Eds.), The Columbia River Estuary and Adjacent Ocean Waters: Bioenvironmental Studies. University of Washington Press, Seattle, Washington.
O'Callaghan, J.F., Mark, D.M., 1984. The extraction of drainage networks from digital elevation data. Comput. Vision Graphics Image Process. 28, 323–344.
Opperman, J.J., Galloway, G.E., Fargione, J., Mount, J.F., Richter, B.D., Secchi, S., 2009. Sustainable floodplains through large-scale reconnection to rivers. Science 326, 1487–1488.
Puget Sound LiDAR Consortium (PSLC). 2005. Lower Columbia River 2005 LiDAR, Final Report. Puget Sound LiDAR Consortium, Seattle, Washington.
Poff, N.L., Allan, J.D., Bain, M.B., Karr, J.R., Prestergaard, K.L., Richter, B.D., Sparks, R.E., Stromberg, J.C., 1997. The natural flow regime: a paradigm for river conservation and restoration. BioScience 47, 769–784.
Polis, G.A., Anderson, W.B., Holt, R.D., 1997. Toward an integration of landscape and food web ecology: the dynamics of spatially subsidized food webs. Annu. Rev. Ecol. System. 18, 289–316.
Poulter, B., Halpin, P.N., 2008. Raster modelling of coastal flooding from sea-level rise. Int. J. Geogr. Inf. Science 22 (1-2), 167–182.
Qian, Y., Gustasfson, W.I., Leung, L.R., Ghan, S.J., 2009. Effects of soot-induced albedo change on snowpack and hydrological cycle in western United States based on weather research forecasting chemistry and regional climate simulations. J. Geophys. Res.-Atmospheres 114, D03108.
Renssen, H., Knoop, J.M., 2000. A global river routing network for use in hydrological modeling. J. Hydrol. 230 (3-4), 230–243.
Riley, S.J., De Gloria, S.D., Elliot, R., 1999. A terrain ruggedness index that quantifies topographic heterogeneity. Intermountain J. Sci. 5 (1–4), 23–27.
Rinaldo, A., Belluco, E., D'Alpaos, A., Feola, A., Lanzoni, S., Marani, M., 2004. Tidal networks: form and function. In: Fagherazzi, S., Marani, M., Blum, L.K. (Eds.), The Ecogeomorphology of Tidal Marshes. American Geophysical Union, Washington, DC.
Russell, G.D., Hawkins, C.P., O'Neill, M.P., 1997. The role of GIS in selecting sites for riparian restoration based on hydrology and land use. Restor. Ecol. 5, 56–68.
Society for Ecological Restoration International (SERI) Science & Policy Working Group, 2004. The SER International Primer on Ecological Restoration. www.ser.org & Tucson AZ: Society for Ecological Restoration International.
Saunders W. 1999. Preparation of DEMs for use in environmental modelling analysis. 1999 ESRI User Conference, ESRI, Online, San Diego, California.
Savant, G., McAlpin, T.O., 2014. Tidal hydrodynamics in the lower Columbia River estuary through depth averaged adaptive hydraulics modeling. J. Eng. Article ID 416914. http://dx.doi.org/10.1155/2014/416914.
Sherwood, C.R., Creager, J.S., 1990. Sedimentary geology of the Columbia River estuary. Prog. Oceanogr 25, 15–79.
Siebentritt, M.A., Ganf, G.G., Walker, K.F., 2004. Effects of an enhanced flood on riparian plants of the River Murray, South Australia. River Res. Appl. 20, 765–774.
Silvestri, S., Defina, A., Marani, M., 2004. Tidal regime, salinity and salt marsh plant zonation. Estuar. Coast. Shelf Sci. 62, 119–130.
Simenstad, C.A., Cordell, J.R., 2000. Ecological assessment criteria for restoring anadromous salmonid habitat in Pacific Northwest estuaries. Ecol. Eng. 15, 283–302.
Simenstad, C.A., Thom, R.M., 1996. Functional equivalency trajectories of the restored Gog-Le-Hi-Te estuarine wetland. Ecol. Appl. 6, 38–56.
Simenstad, C.A., Hood, W.G., Thom, R.M., Levy, D.A., Bottom, D.L., 2000. Landscape structure and scale constraints o restoring estuarine wetlands for Pacific Coast juvenile fishes. In: Weinstein, M.P., Kreeger, D.A. (Eds.), Concepts and Controversies in Tidal Marsh Ecology. Kluwer Academic Publ., Dordrecht, pp. 597–630.
Soille, P., Vogt, J.V., Colombo, R., 2003. Carving and adaptive drainage enforcement of grid digital elevation models. Water Res. Res. 39 (12) 1366–1379.
Tarboton, D.G., 1997. A new method for the determination of flow directions and contributing areas in grid digital elevation models. Water Res. Res. 33 (2), 309–319.
Tesfa, T.K., Tarboton, D.G., Watson, D.W., Schreuders, K.A.T., Baker, M.E., Wallace, R. M., 2011. Extraction of hydrological proximity measures from DEMs using parallel processing. Environ. Model. Software 26, 1696–1709.
Thom, R.M., Diefenderfer, H.L., Adkins, J.E., Judd, C., Anderson, M.G., Buenau, K.E., Borde, A.B., Johnson, G.E., 2012. Guidelines, processes and tools for coastal ecosystem restoration, with examples from the United States. Plankton Benthos Res. (5 (Suppl)), 185–201.
Thomas DW. 1983. Changes in Columbia River Estuary Habitat Types Over the Past Century. Columbia River Estuary Data Development Program 51. Available from Columbia River Estuary Study Taskforce, Box 175, Astoria, Oregon 97103.
Thompson, L., vanManen, F., Shlarbaum, S., DePoy, M., 2006. A spatial modeling approach to identify potential butternut restoration sites in Mammoth Cave National Park. Restor. Ecol. 14, 289–296.
Timm, R.K., Wissmar, R.C., Small, J.W., Leschine, T.M., Lucchetti, G., 2004. A screening procedure for prioritizing riparian management. Environ. Manage. 33, 151–161.
Tockner, K., Stanford, J.A., 2002. Riverine flood plains: present state and future trends. Environ. Conserv. 29, 308–330.
Toth, L.A., 1995. Principles and guidelines for restoration of river/floodplain ecosystems–Kissimmee River, Florida. In: Cairns, J. (Ed.), Rehabilitating Damaged Ecosystems. Lewis Publishers, Boca Raton, pp. 49–73.
Turcotte, R., Fortin, J.P., Rousseau, A.N., Massicotte, S., Villeneuve, J.P., 2001. Determination of the drainage structure of a watershed using a digital elevation model and a digital river and lake network. J. Hydrol. 4, 225–242.
U.S. Army Corps of Engineers (USACE), Columbia River LiDAR Project. CENWP, U.S. Army Corps of Engineers, Portland District, contract No. W9127N-10-D-0002/0001 and W9127N-09-D-0009/0006. Available online: ftp://csc.noaa.gov/pub/DigitalCoast/lidar1_z/geoid12a/data/1122/supplemental/ColumbiaRiverLiDARProject_FinalSummaryReport.doc.
Welcomme, R.L., 1979. Fisheries Ecology of Floodplain Rivers. Longman, London.
Welcomme, R.L., 2008. World prospects for floodplain fisheries. Ecohydrol. Hydrobiol. 8, 169–182.
White, P.S., Pickett, S.T.A., 1985. Natural disturbance and patch dynamics: an introduction. In: Pickett, S.T.A., White, P.S. (Eds.), The Ecology of Natural Disturbance and Patch Dynamics. Academic Press, San Diego, pp. 3–13.
Wozencraft, J.M., Millar, D., 2005. Airborne lidar and integrated technologies for coastal mapping and charting. Marine Technol. Soc. J. 39 (3), 27–35.

Glossary

ATIIM: Area Time Inundation Index Model, a high-resolution spatiotemporal rapid-assessment tool for evaluating patterns of inundation for site-scale restoration and monitoring.

CEERP: Columbia Estuary Ecosystem Restoration Program, a multi-agency ecosystem restoration program within the Lower Columbia River and estuary, located in the northwestern United States.

DEM: Digital Elevation Model, a regularly gridded array of continuous elevation values over a topographic surface and referenced to a common datum.

GIS: Geographic Information System, an integration of software technologies that allow the collection and storage of geographic data, simple to complex spatial analysis, modeling and discovery of geographic phenomena, and map-based visualization of geographic data and analysis.

LCRE: Lower Columbia River and Estuary, the historical floodplain of the lower 234 km of the Columbia River in the northwestern United States including the tidally-influenced main-stem river and tributaries entering the river between the Bonneville Dam the lowest hydroelectric dam on the system, and the river mouth at the Pacific Ocean.

LiDAR: Light Detection and Ranging, a laser-altimeter based airborne remote-sensing system that captures various elevations and intensities from reflective surfaces though vegetation canopy layers through to bare ground. Green-laser systems have the capability to capture ground elevations through water, based on clarity.

NAVD88: North American Vertical Datum of 1988, a vertical datum derived from a geodetic model developed using satellite observation and a single tidal observation station (Father Point, Quebec, Canada) to establish mean sea level.

TIN: Triangulated Irregular Network, A vector data structure that uses XYZ point data to partition geographic space into contiguous, non-overlapping Delaunay triangles. TINs are most commonly used to represent a terrain surface.

WSE: water surface elevation, the stage of the water surface above or below an established datum over a defined measure of time, instantaneous or averaged over time.